AIAA JOURNAL
Vol. 50, No. 6, June 2012

Analysis of Thin-Walled Beam with Crack of Random Location and Size

Chalitphan Kunaporn,* Mahendra P. Singh,† Mayuresh J. Patil,‡ and Rakesh K. Kapania§
Virginia Polytechnic Institute and State University, Blacksburg, Virginia 24061

DOI: 10.2514/1.J051244

This paper presents the analysis of a thin-walled beam with a longitudinal crack of random location and size. The research objective is to understand the response characteristics of such a damaged beam, with the ultimate goal of examining the growth of a crack under random loading. This initial study is expected to guide the future analysis of an aircraft wing with uncertain damage characteristics. An analytical method is presented to obtain the response of a simple thin-walled beam of a closed cross section with a longitudinal crack of finite size. For random location and size of the crack, the methodology for the first-order reliability analysis with analytically calculated response is described. The numerical results of the reliability analysis of the beam for the reliability defined as the nonexceedance of a limit state are presented.

Downloaded by UNIVERSITY OF ILLINOIS on March 7, 2013 | http://arc.aiaa.org | DOI: 10.2514/1.J051244

Nomenclature

A	=	cross-sectional area, m^2
B	=	body force
d_i	=	ith constant of interfacial compatibility
E	=	modulus of elasticity, GPa
G	=	modulus of rigidity, GPa
L_c	=	location of crack, m
L_d	=	size of crack, m
M_x, M_y	=	bending moments about the x and y axes, N · m
M_z	=	torque about the z axis, N · m
M_ω	=	warping moment about the z axis, N · m
m_x, m_y, m_z	=	distributed moments about the x,y, and z axes, N · m/m
m_ω	=	distributed warping moment about the z axis, N · m/m
P_x, P_y	=	shear forces in x and y direction, N
P_z	=	axial force, N
p_x, p_y, p_z	=	distributed force in x, y and z direction, N/m
T	=	traction
u, v	=	x and y displacements in Cartesian coordinate
v_s	=	tangential displacement in normal-tangential coordinate
w	=	warping displacement of contour origin
γ_{sz}	=	shear strain in s–z plane
γ_{xz}, γ_{yz}	=	shear strains in x–z and y–z planes
θ_x, θ_y	=	pole rotation about the x and y axes
θ_z	=	angle of twist about the z axis
θ'_z	=	rate of twist about the z axis
ϕ	=	measure of warping
ε_{zz}	=	normal strain in the z direction
ψ	=	warping function

Presented at the 51st AIAA/ASME/ASCE/AHS/ASC Structures, Structural Dynamics, and Materials Conference, Orlando, FL, 12–15 April 2010; received 7 March 2011; revision received 1 August 2011; accepted for publication 8 December 2011. Copyright © 2011 by the authors. Published by the American Institute of Aeronautics and Astronautics, Inc., with permission. Copies of this paper may be made for personal or internal use, on condition that the copier pay the $10.00 per-copy fee to the Copyright Clearance Center, Inc., 222 Rosewood Drive, Danvers, MA 01923; include the code 0001-1452/12 and $10.00 in correspondence with the CCC.

*Graduate Research Assistant, Department of Engineering Mechanics; kunaporn@vt.edu. Member AIAA.
†Preston Wade Professor, Department of Engineering Mechanics; mpsingh@vt.edu.
‡Associate Professor, Department of Aerospace and Ocean Engineering; mpatil@vt.edu. Senior Member AIAA.
§Mitchell Professor, Department of Aerospace and Ocean Engineering; rkapania@vt.edu. Associate Fellow AIAA.

I. Introduction

THE damage in a wing can significantly affect the performance of an aircraft. With the motivation of examining the performance of an aircraft with a damaged wing, this study examines the response of a hollow thin-walled beam with a longitudinal crack. The crack location and size are considered random. First, the paper presents an analytical formulation to obtain the response of the beam as a function of the crack parameters followed by probabilistic and reliability analysis.

The currently available thin-walled-beam theories are adequate to model beams without a crack and are able to provide accurate values of the overall response. They require appropriate modifications to include a crack, and such modifications are described in this study. These modifications are able to accurately capture the effect of a crack on the overall deformation response such as displacements and angle of twist, but not the stresses near the crack. So this study focuses primarily on the overall deformation analysis of such a beam.

A beam with a longitudinal crack can be represented by three interconnected thin-walled beams. The portion of the beam with the crack can be modeled as an open-section thin-walled beam, whereas the other two sections are closed-section thin-walled beams. When subjected to lateral loads or a twisting moment, such a beam is expected to warp. The thin-walled-beam theories that allow us to include warping can be mainly divided into two categories: Vlasov beam theory [1–5] and Benscoter beam theory [1–7]. In this study, the derivation is based on Benscoter beam theory, where the warping degree of freedom is considered to be independent of the rate of twist. This independence between the warping and the rate of twist allows us the use of the method of least-squares compatibility (introduced by Gunnlaugsson and Pedersen [2]) to effectively treat the discontinuity between cracked and uncracked cross sections without requiring the use of complicated warping functions [8,9]. The equilibrium equations and the boundary conditions for the system are derived using the principle of virtual work. The coupled equilibrium equations are then expressed in state-space form, which allows us to solve them using the Jordan canonical-form approach. The accuracy of the calculated response by the proposed approach is verified by a detailed shell finite element analysis.

To investigate the effect of random characteristics of a crack on the performance, a first-order reliability analysis method [10–14] is used. The higher-order analyses [15] could also be used to improve the reliability estimates, especially if the limit-state boundary is highly nonlinear. This is not attempted in this study, however, as the limit-state boundaries used in this study are nearly linear. For the reliability analysis, the limit state is defined in terms of the angle of twist exceeding some limiting value. Although the response quantity of interest is not explicitly defined in terms of the crack parameters, surrogate methods such as response-surface approaches [16,17] are

Downloaded by UNIVERSITY OF ILLINOIS on March 7, 2013 | http://arc.aiaa.org | DOI: 10.2514/1.J051244

not needed in this case, as the gradients needed for the reliability analysis can still be calculated by the chain rule and applied at successive analytical steps that are used in the response calculations. Publications in this area of interest are, for example, [18–20].

II. Analytical Model of a Thin-Walled Beam with a Crack

The damaged structure is modeled as a hollow cantilever thin-walled beam of a rectangular shape, shown in Fig. 1. The damage is represented by a longitudinal crack of a given length on the top face. The beam is divided into three parts, with the cracked part between the two undamaged parts. The undamaged beam portions are represented as closed-cross-section thin-walled beam, and the damaged portion as the open-cross-section thin-walled beam, as shown in Fig. 1. The kinematics of thin-walled beam are described using the combination of the Cartesian (x, y, z) coordinates and orthogonal curvilinear (s, n, z) coordinates. For convenience, the global (Z) and local (z_i) coordinates are used interchangeably.

The closed cross section is assumed to be not deformable in its own plane. Therefore, only rigid-body motions are allowed for the in-plane displacements. The warping in both cross sections introduces axial deformations along the z direction and shear deformations in the plane of the cross section. As shown in Fig. 2, an arbitrary point $P(x_p, y_p)$, or so-called pole, is used as the reference point to describe all displacement fields. The pole of a cross section along the beam span is chosen at the shear centers, and the angle of twist θ_z is assumed to be about this point. Only two coordinates (θ_z and warping displacement w) are needed to define the displacement and stress field to derive the governing equations. The tangential displacements v_s and the out-of-plane warping displacement w are used to define the displacement field in the (s, n, z) coordinate system. To calculate the warping function of a thin-walled section, we choose a reference point $CO(x_{co}, y_{co})$, where the coordinate $s = 0$ for contour integration. The dimensions b and h, respectively, are the width and height of the beam cross section.

An additional degree of freedom, $\phi(z)$, is introduced as the measure of warping. As in Benscoter's thin-walled-beam theory [1], it is assumed to be independent of the axial rotation degree of freedom of the beam. In terms of these kinematics parameters, the tangential and warping displacements can now be written as follows [2]:

$$v_s(s, n, z) = u(z)\frac{\partial x(s)}{\partial s} + v(z)\frac{\partial y(s)}{\partial s} + r_n(s, n)\theta_z(z) \tag{1}$$

$$w(s, n, z) = w_o(z) + y(s)\theta_x(z) - x(s)\theta_y(z) - \psi(s, n)\phi(z) \tag{2}$$

where $u(z)$ and $v(z)$ are the displacements of the pole in the x and y directions, respectively; $w_o(z)$ is the warping displacement of the contour origin; $\theta_x(z)$ and $\theta_y(z)$ are the rotations of the pole with respect to the x and y axes, respectively; $\theta_z(z)$ is the angle of twist; $\psi(s, n)$ is the warping function; $\phi(z)$ is the measure of warping that can be approximated to the rate of twist, in special cases; $(\,)'$ denotes the derivative with respect to z; and $x(s)$ and $y(s)$ are Cartesian coordinate rewritten in terms of the tangential coordinate. In the linear theory, the rotations of pole are described as follows:

$$\theta_x(z) = \gamma_{yz}(z) - v'(z) \tag{3}$$

$$\theta_y(z) = \gamma_{xz}(z) - u'(z) \tag{4}$$

where γ_{xz} and γ_{yz} are transverse strains.

In the shear deformable beam theory, the Euler–Bernoulli hypothesis is no longer applicable, as $\gamma_{xz} \neq 0$ and $\gamma_{yz} \neq 0$ and the transverse strains are included in the derivation. The infinitesimal strain tensor in linear theory is expressed in terms of displacements. Based on the thin-walled theory, the energy equation requires only two main strain components: ε_{zz}, which is the normal strain in the z direction, and $\gamma_{sz} = 2\varepsilon_{sz}$, which is the shear strain in the s–z plane. They are defined as follows:

$$\varepsilon_{zz} = \frac{\partial w}{\partial z} \tag{5}$$

$$\gamma_{sz} = 2\varepsilon_{sz} = \frac{\partial v_s}{\partial z} + \frac{\partial w}{\partial s} \tag{6}$$

Both the open and the two closed cross sections have the same geometric center, but different shear centers, thus causing the centers of twist to be different for the three sections. Although the beam is subjected only to torsion, it is no longer the case of pure torsion, but the coupled bending and torsion must be considered. The governing equations are derived using the principle of virtual work. The following derivation is based on isotropic materials; however, it could be generalized to use for the composite materials, see [21]. In static analysis, the principle of virtual work can be written as

$$\delta W_{\text{Internal Work}} - \delta W_{\text{External Work}} = 0 \tag{7}$$

$$\iiint_V \sigma\delta\varepsilon \,\mathrm{d}V - \left(\iiint_V B\delta u \,\mathrm{d}V + \iint_S T\delta u \,\mathrm{d}S\right) = 0 \tag{8}$$

where B and T stand for the body forces and the tractions, respectively.

For a thin-walled-beam cross section, the body forces are zero in a static case and the term of work due to strain energy can be simplified. Considering the tractions in the form of distributed loads along the span and concentrated loads at certain locations of the span, the principle of virtual work can be written as follows:

$$\int_0^L \left[\int_A (E\varepsilon_{zz}\delta\varepsilon_{zz} + G\gamma_{sz}\delta\gamma_{sz})\,\mathrm{d}A - (p_x\delta u + p_y\delta v + p_z\delta w + m_x\delta\theta_y + m_y\delta\theta_x + m_z\delta\theta_z - m_\omega\delta\phi)\right]\mathrm{d}Z - (P_x\delta u + P_y\delta v + P_z\delta w + M_x\delta\theta_x + M_y\delta\theta_y + M_z\delta\theta_z - M_\omega\delta\phi)|_{Z=Z_l} = 0 \tag{9}$$

where E is Young's modulus; G is the modulus of torsional rigidity; p_x, p_y, and p_z are the distributed forces in the x, y, and z directions,

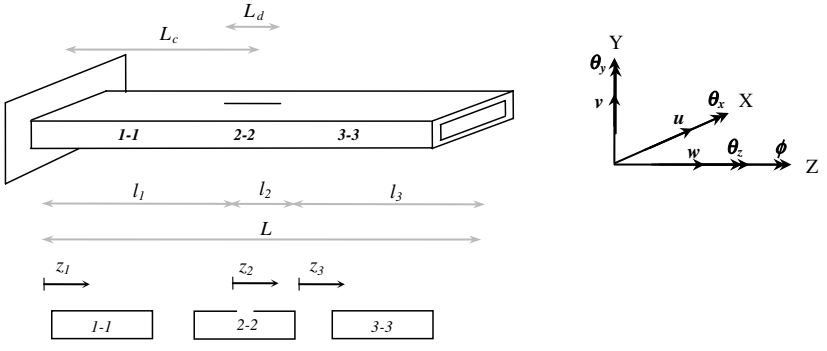

Fig. 1 Damaged structure modeled with a cracked thin-walled cantilever.

respectively; m_x, m_y, and m_z are the distributed moments with respect to the x, y, and z axes, respectively; and m_ω is the distributed warping torque about the z axis; P_x and P_y are the shear forces in the x and y directions, respectively; P_z is the axial force; M_x and M_y are the bending moments with respect to the x and y axes, respectively; M_z is the torque; M_ω is the warping moment or the so-called bimoment; and Z_l is the location of concentrated load that can be between 0 and L.

In the spanwise direction, the beam model consists of three portions. For convenience, the local coordinates are mainly used as the references in the spanwise direction. The first portion has boundaries from $z_1 = 0$ to $z_1 = l_1$, the second portion with the crack spans from $z_2 = 0$ to $z_2 = l_2$, and the last portion spans from $z_3 = 0$ to $z_3 = l_3$. For the plane of cross section, however, the global coordinates are still used. The contour origin is chosen so that the warping displacement of the contour origin, $w_o(z)$, is zero. Substituting all stress and strain components and applying the principle of virtual work, the system of equilibrium equations and the corresponding boundary-continuity conditions are obtained as follows:

$$-EAw'' = p_z \tag{10}$$

$$-GJ_{\theta y}\theta_z'' + GQ_{yz}\phi' - GQ_{xy}(v'' + \theta_x') - GQ_{yy}(u'' - \theta_y') = p_x \tag{11}$$

$$-GJ_{\theta x}\theta_z'' + GQ_{xz}\phi' - GQ_{xx}(v'' + \theta_x') - GQ_{xy}(u'' - \theta_y') = p_y \tag{12}$$

$$E\Gamma_{zx}\phi'' - EI_{xx}\theta_x'' + EI_{xy}\theta_y'' + GJ_{\theta x}\theta_z' - GQ_{xz}\phi + GQ_{xx}(v' + \theta_x) + GQ_{xy}(u' - \theta_y) = m_x \tag{13}$$

$$-E\Gamma_{zy}\phi'' + EI_{xy}\theta_x'' - EI_{yy}\theta_y'' - GJ_{\theta y}\theta_z' + GQ_{yz}\phi - GQ_{xy}(v' + \theta_x) - GQ_{yy}(u' - \theta_y) = m_y \tag{14}$$

$$-GJ_{\theta\theta}\theta_z'' + GJ_{\theta z}\phi' - GJ_{\theta x}(v'' + \theta_x') - GJ_{\theta y}(u'' - \theta_y') = m_z \tag{15}$$

$$-E\Gamma_{zz}\phi'' + E\Gamma_{zx}\theta_x'' - E\Gamma_{zy}\theta_y'' - GJ_{\theta z}\theta_z' + GJ_{zz}\phi - GQ_{xz}(v' + \theta_x) - GQ_{yz}(u' - \theta_y) = -m_\omega \tag{16}$$

The geometric problem parameters used in the above equations are defined as follows:

$$A = \int_A \mathrm{d}A, \qquad S_{xx} = \int_A y\,\mathrm{d}A, \qquad S_{yy} = \int_A x\,\mathrm{d}A$$

$$S_{zz} = \int_A \psi\,\mathrm{d}A \qquad \Gamma_{zz} = \int_A \psi^2\,\mathrm{d}A, \qquad \Gamma_{zx} = \int_A y\psi\,\mathrm{d}A$$

$$\Gamma_{zy} = \int_A x\psi\,\mathrm{d}A, \qquad I_{xx} = \int_A y^2\,\mathrm{d}A, \qquad I_{xy} = \int_A xy\,\mathrm{d}A$$

$$I_{yy} = \int_A x^2\,\mathrm{d}A \qquad J_{\theta\theta} = \int_A R_n^2\,\mathrm{d}A, \qquad J_{\theta z} = \int_A R_n\frac{\partial\psi}{\partial s}\,\mathrm{d}A$$

$$J_{zz} = \int_A \left(\frac{\partial\psi}{\partial s}\right)^2\mathrm{d}A, \qquad J_{\theta x} = \int_A R_n\frac{\partial y}{\partial s}\,\mathrm{d}A$$

$$J_{\theta y} = \int_A R_n\frac{\partial x}{\partial s}\,\mathrm{d}A \qquad Q_{xx} = \int_A \left(\frac{\partial y}{\partial s}\right)^2\mathrm{d}A$$

$$Q_{xy} = \int_A \frac{\partial x}{\partial s}\frac{\partial y}{\partial s}\,\mathrm{d}A, \qquad Q_{yy} = \int_A \left(\frac{\partial x}{\partial s}\right)^2\mathrm{d}A$$

$$Q_{xz} = \int_A \frac{\partial y}{\partial s}\frac{\partial\psi}{\partial s}\,\mathrm{d}A, \qquad Q_{yz} = \int_A \frac{\partial x}{\partial s}\frac{\partial\psi}{\partial s}\,\mathrm{d}A$$

The corresponding boundary conditions at the two ends are obtained as shown next.

At the fixed end, $Z = 0$,

$$u = 0, \qquad v = 0, \qquad w = 0 \tag{17}$$

$$\theta_x = 0, \qquad \theta_y = 0, \qquad \theta_z = 0 \tag{18}$$

$$\phi = 0 \tag{19}$$

At the free end, $Z = L$,

$$GJ_{\theta y}\theta_z' - GQ_{yz}\phi + GQ_{xy}(v' + \theta_x) + GQ_{yy}(u' - \theta_y) = P_x \tag{20}$$

$$GJ_{\theta x}\theta_z' - GQ_{xz}\phi + GQ_{xx}(v' + \theta_x) + GQ_{xy}(u' - \theta_y) = P_y \tag{21}$$

$$EAw' = P_z \tag{22}$$

$$-E\Gamma_{zx}\phi' + EI_{xx}\theta_x' - EI_{xy}\theta_y' = M_x \tag{23}$$

$$E\Gamma_{zy}\phi' + EI_{xy}\theta_x' - EI_{yy}\theta_y' = M_y \tag{24}$$

$$GJ_{\theta\theta}\theta_z' - GJ_{\theta z}\phi + GJ_{\theta x}(v' + \theta_x) + GJ_{\theta y}(u' - \theta_y) = M_z \tag{25}$$

$$E\Gamma_{zz}\phi' - E\Gamma_{zx}\theta_x' - E\Gamma_{zy}\theta_y' = -M_\omega \tag{26}$$

At the interface of the uncracked and cracked portions of the beam, the boundary conditions are defined in terms of the continuity conditions, as described in the following.

A. Continuity Conditions

Because of different warping functions used between the closed and the open cross sections, the discontinuity of warping displacements at the interface of the two sections across the beam portion is inevitable. To deal with this issue, the thin-walled-beam theory is modified by incorporating the technique proposed by Gunnlaugsson and Pedersen [2,3] to account for the compatibility conditions in the standard governing equations. To facilitate the minimization of the difference, they proposed to include additional constants in the representation of the warping displacement only on one side of the interface, as explained in the following.

At the interface of the two different cross sections, the warping displacement field of the element on the right-hand side is rewritten to include the assumed compatibility constants as follows:

$$w^{\text{right}}(s,n,z) = w_o(z) + y(s)\theta_x(z) - x(s)\theta_y(z) - [d_1 + d_2 y(s) - d_3 x(s) + d_4\psi^{\text{right}}(s,n)]\phi(z) \tag{27}$$

whereas the warping displacement of the right element remains unchanged as

$$w^{\text{left}}(s,n,z) = \bar{w}(z) + y(s)\theta_x(z) + x(s)\theta_y(z) - \psi^{\text{left}}(s,n)\phi(z) \tag{28}$$

The compatibility constants d_i are assumed to be associated with the measure of warping degree of freedom $\phi(z)$, while each of them relates to each cross section's dimension. Detailed descriptions can be found in [2,3]. To calculate these constants and define the

Downloaded by UNIVERSITY OF ILLINOIS on March 7, 2013 | http://arc.aiaa.org | DOI: 10.2514/1.J051244

compatibility condition, we minimize the following integral norm of the pointwise difference between the warping displacements:

$$I = \int_A (w^{\text{left}} - w^{\text{right}})^2 \, \mathrm{d}A \tag{29}$$

where the superscripts left and right denote the closed and open cross sections, respectively.

The necessary conditions for the minimization of this functional provide the compatibility conditions and the following four equations to calculate the constant d_i:

$$\frac{\partial I}{\partial d_1} = 0\text{:} \int_A (w^{\text{left}} - w^{\text{right}}) \, \mathrm{d}A = 0 \tag{30}$$

$$\frac{\partial I}{\partial d_2} = 0\text{:} \int_A (w^{\text{left}} - w^{\text{right}}) y \, \mathrm{d}A = 0 \tag{31}$$

$$\frac{\partial I}{\partial d_3} = 0\text{:} \int_A (w^{\text{left}} - w^{\text{right}}) x \, \mathrm{d}A = 0 \tag{32}$$

$$\frac{\partial I}{\partial d_4} = 0\text{:} \int_A (w^{\text{left}} - w^{\text{right}}) \psi^{\text{right}} \, \mathrm{d}A = 0 \tag{33}$$

On expansion, the above equations at each interface between the discontinuous sections lead to the following four simultaneous equations for calculating the constants d_i expressed in terms of the integration constants of the beam cross sections:

$$d_1 A^{\text{right}} + d_2 S_{xx}^{\text{right}} - d_3 S_{yy}^{\text{right}} + d_4 S_{zz}^{\text{right}} = S_{zz}^{\text{left}} \tag{34}$$

$$d_1 S_{xx}^{\text{right}} + d_2 I_{xx}^{\text{right}} - d_3 I_{xy}^{\text{right}} + d_4 \Gamma_{zx}^{\text{right}} = \Gamma_{zx}^{\text{left}} \tag{35}$$

$$d_1 S_{yy}^{\text{right}} + d_2 I_{xy}^{\text{right}} - d_3 I_{yy}^{\text{right}} + d_4 \Gamma_{zy}^{\text{right}} = \Gamma_{zy}^{\text{left}} \tag{36}$$

$$d_1 S_{zz}^{\text{right}} + d_2 \Gamma_{zx}^{\text{right}} - d_3 \Gamma_{zy}^{\text{right}} + d_4 \Gamma_{zz}^{\text{right}} = \Gamma_{zzlr} \tag{37}$$

where the integration constants of the beam cross section (A, S_{xx}, S_{yy}, S_{zz}, I_{xx}, I_{xy}, I_{yy},Γ_{zz}, Γ_{zx}, and Γ_{zy}) are the same as defined earlier after the equilibrium equations, but they are now defined separately for the left and right parts of the beam cross sections. See Table 3 for a list of the cross section's constants. Another constant, undefined earlier, is

$$\Gamma_{zzlr} = \int_A \psi^{\text{left}} \psi^{\text{right}} \, \mathrm{d}A$$

which uses the warping function on the left- and right-hand-side cross sections.

Here, it is noted that all integration constants are calculated using the shear centers as references for both cross sections. At this step, the constants obtained using the pole as the references cannot be used because of the flexural–torsional coupling. However, in order to obtain the unique values of all constants, no matter which element is assumed to be on the left-hand or the right-hand sides, an additional normalization needs to be implemented. It requires that the product of both constants d_4 (one when the closed cross section is on the left and the other when the closed cross section is on the right) be normalized. This is essentially equivalent to the orthogonality, as explained in [3]. The compatibility constants can be implemented into the model directly as follows:

$$u|_{\text{left}} = u|_{\text{right}} \tag{38}$$

$$v|_{\text{left}} = v|_{\text{right}} \tag{39}$$

$$w|_{\text{left}} + d_1 \phi|_{\text{left}} = w|_{\text{right}} \tag{40}$$

$$\theta_x|_{\text{left}} + d_2 \phi|_{\text{left}} = \theta_x|_{\text{right}} \tag{41}$$

$$\theta_y|_{\text{left}} - d_3 \phi|_{\text{left}} = \theta_y|_{\text{right}} \tag{42}$$

$$\theta_z|_{\text{left}} = \theta_z|_{\text{right}} \tag{43}$$

$$d_4 \phi|_{\text{left}} = \phi|_{\text{right}} \tag{44}$$

$$P_x|_{\text{left}} = P_x|_{\text{right}} \tag{45}$$

$$P_y|_{\text{left}} = P_y|_{\text{right}} \tag{46}$$

$$P_z|_{\text{left}} = P_z|_{\text{right}} \tag{47}$$

$$M_x|_{\text{left}} = M_x|_{\text{right}} \tag{48}$$

$$M_y|_{\text{left}} = M_y|_{\text{right}} \tag{49}$$

$$M_z|_{\text{left}} = M_z|_{\text{right}} \tag{50}$$

$$-M_\omega|_{\text{left}} = d_1 P_Z|_{\text{right}} + d_2 M_x|_{\text{right}} + d_3 M_y|_{\text{right}} - d_4 M_\omega|_{\text{right}} \tag{51}$$

III. Analytical Solutions

A. Solution Approach

To obtain the analytical solution for the general case, we rewrite the set of equations as a set of coupled first-order equations using state variables. For this, the following auxiliary variables are introduced: $u_1 = u'$, $v_1 = v'$, $\theta_{x1} = \theta_x'$, $\theta_{y1} = \theta_y'$, $\theta_{z1} = \theta_z'$, and $\phi_1 = \phi'$, where prime denotes the derivative with respect to z; w is automatically uncoupled and is thus not included in the analysis. The state vector of variables is defined as

$$\underline{X} = \lfloor u \quad u_1 \quad v \quad v_1 \quad \theta_x \quad \theta_{x1} \quad \theta_y \quad \theta_{y1} \quad \theta_z \quad \theta_{z1} \quad \phi \quad \phi_1 \rfloor^T$$

With the assignment of auxiliary variables as indicated above, the coupled equations can be rewritten in the state form as

Downloaded by UNIVERSITY OF ILLINOIS on March 7, 2013 | http://arc.aiaa.org | DOI: 10.2514/1.J051244

$$
\begin{bmatrix}
1 & & & & & & & & & & & \\
-GQ_{yy} & & -GQ_{xy} & & & & & -GJ_{\theta y} & & & & \\
& 1 & & & & & & & & & & \\
-GQ_{xy} & & -GQ_{xx} & & & & & -GJ_{\theta x} & & & & \\
& & & 1 & & & & & & & & \\
& & & & -EI_{xx} & & EI_{xy} & & & & E\Gamma_{zx} & \\
& & & & & 1 & & & & & & \\
& & & & EI_{xy} & & -EI_{yy} & & & & -E\Gamma_{zy} & \\
& & & & & & & 1 & & & & \\
-GJ_{\theta y} & & -GJ_{\theta x} & & & & & -GJ_{\theta\theta} & & & & \\
& & & & & & & & 1 & & & \\
& & & & E\Gamma_{zx} & & -E\Gamma_{zy} & & & & -E\Gamma_{zz} &
\end{bmatrix}
\begin{bmatrix} u' \\ u'_1 \\ v' \\ v'_1 \\ \theta'_x \\ \theta'_{x1} \\ \theta'_y \\ \theta'_{y1} \\ \theta'_z \\ \theta'_{z1} \\ \phi' \\ \phi'_1 \end{bmatrix}
$$

$$
= \begin{bmatrix}
1 & & & & & & & & & & & \\
& & & & GQ_{xy} & & -GQ_{yy} & & & & -GQ_{yz} & \\
& & 1 & & & & & & & & & \\
& & & & GQ_{xx} & & -GQ_{xy} & & & & -GQ_{xz} & \\
& & & & & 1 & & & & & & \\
-GQ_{xy} & -GQ_{xx} & -GQ_{xx} & & GQ_{xy} & & & -GJ_{\theta x} & GQ_{xz} & & & \\
& & & & & & 1 & & & & & \\
GQ_{yy} & GQ_{xy} & GQ_{xy} & & -GQ_{yy} & & & GJ_{\theta y} & -GQ_{yz} & & & \\
& & & & & & & 1 & & & & \\
& & & & GJ_{\theta x} & & -GJ_{\theta y} & & & & -GJ_{\theta z} & \\
& & & & & & & & & 1 & & \\
GQ_{yz} & GQ_{xz} & GQ_{xz} & GJ_{\theta z} & -GQ_{yz} & & & & -GJ_{zz} & &
\end{bmatrix}
\begin{bmatrix} u \\ u_1 \\ v \\ v_1 \\ \theta_x \\ \theta_{x1} \\ \theta_y \\ \theta_{y1} \\ \theta_z \\ \theta_{z1} \\ \phi \\ \phi_1 \end{bmatrix}
+ \begin{bmatrix} 0 \\ p_x \\ 0 \\ p_y \\ 0 \\ m_x \\ 0 \\ m_y \\ 0 \\ m_z \\ 0 \\ -m_\omega \end{bmatrix}
\tag{52}
$$

Equation (52) yields the first-order ordinary differential equation (ODE) in the form

$$\underline{A}\underline{X}' = \underline{B}\,\underline{X} + \underline{F} \tag{53}$$

$$\underline{X}' = \underline{A}^{-1}\underline{B}\,\underline{X} + \underline{A}^{-1}\underline{F} \tag{54}$$

To obtain the solution of such equation, one can use the eigenfunction expansion approach. This approach would need to be modified, however, to deal with the zero or repeated eigenvalues of the state equations that could occur in this case. Such modifications can be conveniently affected by the use of the Jordan canonical form of the system following Weintraub [22]. Here, the Jordan matrix and the corresponding matrix of transformation are represented by $\underline{J}$ and $\underline{\phi}$, respectively. Let us define

$$\underline{X} = \underline{\Phi}\,\underline{Q} \tag{55}$$

Substituting Eq. (55) into Eq. (54), we obtain

$$\underline{\Phi}\underline{Q}' = \underline{A}^{-1}\underline{B}\,\underline{\Phi}\,\underline{Q} + \underline{A}^{-1}\underline{F} \tag{56}$$

Premultiplying Eq. (56) by $\underline{\Phi}^{-1}$, we obtain

$$\underline{\Phi}^{-1}\underline{\Phi}\underline{Q}' = \underline{\Phi}^{-1}\underline{A}^{-1}\underline{B}\,\underline{\Phi}\,\underline{Q} + \underline{\Phi}^{-1}\underline{A}^{-1}\underline{F} \tag{57}$$

Consequently,

$$\underline{Q}' = \underline{J}\,\underline{Q} + \underline{E} \tag{58}$$

where $\underline{\Phi}^{-1}\underline{\Phi} = I$, $\underline{\Phi}^{-1}\underline{A}^{-1}\underline{B}\,\underline{\Phi} = \underline{J}$, and $\underline{\Phi}^{-1}\underline{A}^{-1}\underline{F} = \underline{E}$.

The final solution of the ODE in Eq. (58) is typically written as the combination of homogeneous and particular solution as

$$\underline{X} = \underline{X}_P + \underline{X}_H \tag{59}$$

The particular and homogeneous solution in this equation can be expressed as

$$\underline{X}_P = \underline{\Phi}\,\underline{M(z)} \int_0 \underline{M(z)}^{-1}\underline{E}\,\mathrm{d}z \tag{60}$$

$$\underline{X}_H = \underline{\Phi}\,\underline{M(z)}\,\underline{c} \tag{61}$$

where $\underline{M(z)}$ and $\underline{c}$ are the matrix of functions and the vector of the constants of integration, respectively. The details of various matrices and vectors are provided in Appendix A. Substituting these forms of particular and homogeneous solutions in Eq. (59), we obtain the following for the complete solution:

$$\underline{X} = \underline{\Phi}[\underline{I(z)} + \underline{d(z)}] \tag{62}$$

where

$$\underline{I(z)} = \underline{M(z)} \int_0 \underline{M(z)}^{-1}\underline{E}\,\mathrm{d}z$$

and

$$\underline{d(z)} = \underline{M(z)}\,\underline{c}$$

Using this solution, all response quantities related to the state vector can thus be written in analytical form. For example, the angle of twist and deflection in the ith beam section, respectively, are given as

$$\theta_z^{(i)} = \sum_{k=1}^{n} \Phi_{7k}^{(i)}[I_k^{(i)}(z) + d_k^{(i)}(z)] \tag{63}$$

$$u^{(i)} = \sum_{k=1}^{n} \Phi_{1k}^{(i)}[I_k^{(i)}(z) + d_k^{(i)}(z)] \tag{64}$$

where n is the dimension of the state equation, which is $n = 12$ in this case.

To obtain the constants of integration in vector $\underline{c}$, we need to apply the boundary and continuity conditions in each portion of the beam. For each section, the vector $\underline{c}$ consists of 12 constants of integration. Thus, for a three-section beam, there are 36 such constants of integration. In addition, there are four constants d_i that were introduced in enforcing the warping displacement compatibilities at each section interface. With two section interfaces, this introduced eight more constants to be calculated. Thus, a three-section beam will

Downloaded by UNIVERSITY OF ILLINOIS on March 7, 2013 | http://arc.aiaa.org | DOI: 10.2514/1.J051244

require the calculation of a total of 44 constants. The six boundary equations (17–19) at the fixed end; six boundary Eqs. (20–26), excluding Eq. (22) at the free end; four minimization conditions (34–37) at each interface; and 12 additional conditions in equations (38–51), excluding Eqs. (40) and (47) at each interface provide just the right number of equations to calculate all constants of integration in vector $\underline{c}$ and d_i. Application of these boundary conditions leads to the following simultaneous equations to solve for the constants:

$$\underline{G}\,\underline{c} = \underline{F}_G \tag{65}$$

The details of the elements of the matrix $\underline{G}$ and vectors $\underline{c}$ and $\underline{F}_G$ in Eq. (65) are provided in Appendix B. Knowing these constants, one can obtain any response quantity of interest that can be defined in terms of the state vectors. This expression is used in the probabilistic analysis in the following section.

B. Probabilistic Analysis

In this section, the safety-index approach used to evaluate the effect of the presence of a crack on the system performance in probabilistic terms is briefly described. It is assumed that the crack length L_d and its location L_c along the beam are random quantities defined by two independent random variables. Other problem parameters such as cross-sectional dimensions and the applied load could also be assumed to be random quantities. However, to simplify the formulation and to demonstrate the methodology, it is assumed that just these two crack parameters are random variables. To evaluate probabilistic performance, a limit state is defined for which the performance of the system is examined. The limit state could be defined in terms of a stress or a deformation quantity exceeding the allowable values. Herein, for demonstration, the failure limit state is defined as the angle of twist at the free end in the damaged beam exceeding the angle of twist at the same point in the uncracked beam, $\bar{\theta}^{\text{tip}}$, by a fraction α. This condition can thus be stated as $\theta^{\text{tip}} > (1+\alpha)\bar{\theta}^{\text{tip}}$. The corresponding limit-state boundary for safety analysis is then defined as follows:

$$g(L_c, L_d) = (1+\alpha)\bar{\theta}^{\text{tip}} - \theta^{\text{tip}} \tag{66}$$

where $g(L_c, L_d) > 0$ implies safety and $g(L_c, L_d) \leq 0$ as the failure. The angle of twist at the tip of the cracked beam, θ^{tip}, is defined by Eq. (63) above.

To obtain the probability of failure or survival, the probability distributions of the variables that define the limit state are required to calculate the probability mass over the corresponding domains. Often, however, it is not possible to have reliable information about the distribution of the variables and only the first two moments (mean and variance) can be reliably obtained. Even if the distribution information were available, it is often very difficult to calculate the probability mass over the survival or failure domains, if the limit state is nonlinear. Methods have been developed to improve the accuracy for such calculations. The main difficulty, however, remains in defining the distributions of the random variables. With the limited information available about the first two moments, one can obtain a good measure of the reliability in terms of the safety index. If the involved variables can also be assumed to be Gaussian random variables, then the safety index provides the exact value of the probability if the limit-state boundary is linear and approximate value if the limit-state boundary is nonlinear. The approaches to calculate the safety index and the probability of failure for a given limit state are well established. In the following, it is assumed that the mean and standard deviation values of the two random variables that define the crack parameters are known. To calculate the safety index conveniently, the well-known Rackwitz and Fiessler [10–12] iterative algorithm is implemented. This algorithm calculates the design point, which is the closest point to the limit-state boundary in the reduced space of the variables. The coordinates of the design point in the space of the variables are defined as follows:

$$L_c^* = \mu_c + \beta\alpha_c\sigma_c, \qquad L_d^* = \mu_d + \beta\alpha_d\sigma_d \tag{67}$$

where an asterisk denotes the design-point value of the variables; μ_c and σ_c are the mean and standard deviation values of the crack location L_c; μ_d and σ_d are mean and standard deviation values of the of crack length L_d; β is the safety index; and α_c and α_d are direction cosines of the perpendicular to the limit state at the design point. These direction cosines are defined as follows:

$$\alpha_c = \left.\frac{-\sigma_c \frac{\partial g}{\partial L_c}}{\sqrt{\sigma_c^2(\frac{\partial g}{\partial L_c})^2 + \sigma_d^2(\frac{\partial g}{\partial L_d})^2}}\right|_{L_c^*, L_d^*} \tag{68}$$

$$\alpha_d = \left.\frac{-\sigma_d \frac{\partial g}{\partial L_d}}{\sqrt{\sigma_c^2(\frac{\partial g}{\partial L_c})^2 + \sigma_d^2(\frac{\partial g}{\partial L_d})^2}}\right|_{L_c^*, L_d^*} \tag{69}$$

The safety index, as the shortest distance in the reduced space, is thus defined as follows:

$$\beta = [((L_c^* - \mu_c)/\sigma_c)^2 + ((L_d^* - \mu_d)/\sigma_d)^2] \tag{70}$$

For nonlinear limit states, the calculation of the safety index is an iterative process in which appropriate values are assumed for the design point at which the gradients and direction cosines are calculated. The design point defined by Eq. (67) lies on the limit state. Thus, substitution of Eq. (67) in the limit state and solving for the safety index provides the first value of the safely index. This value is used in Eq. (67) to obtain the new design point and the process is repeated. The convergence is fast in most cases. The gradients of the limit-state function required in Eqs. (68) and (69) are obtained by the chain rule of differentiation. For example, the partial derivatives of the limit-state function with respect to the variables L_c and L_d required in Eqs. (68) and (69) are defined as follows:

$$\frac{\partial g}{\partial L_c} = -\frac{\partial \theta^{\text{tip}}}{\partial L_c} = -\sum_{m=1}^{3} \frac{\partial \theta^{\text{tip}}}{\partial l_m}\frac{\partial l_m}{\partial L_c} \tag{71}$$

$$\frac{\partial g}{\partial L_d} = -\frac{\partial \theta^{\text{tip}}}{\partial L_d} = -\sum_{m=1}^{3} \frac{\partial \theta^{\text{tip}}}{\partial l_m}\frac{\partial l_m}{\partial L_d} \tag{72}$$

where l_1, l_2, and l_3 are the variables of the coordinates of ends of the three beam sections shown in Fig. 1. These coordinates can be expressed in terms of the random parameters of the crack, L_c and L_d, as follows:

$$l_1 = L_c - \frac{L_d}{2}, \qquad l_2 = L_d, \qquad l_3 = l - L_c + \frac{L_d}{2} \tag{73}$$

The partial derivatives, appearing in Eqs. (71) and (72), are defined in terms of the following partials used in the chain rule.

Derivatives of l_m ($m = 1, 2, 3$) are as follows:

$$\frac{\partial l_1}{\partial L_c} = 1, \qquad \frac{\partial l_2}{\partial L_c} = 0, \qquad \frac{\partial l_3}{\partial L_c} = -1 \tag{74}$$

$$\frac{\partial l_1}{\partial L_d} = -\frac{1}{2}, \qquad \frac{\partial l_2}{\partial L_d} = 1, \qquad \frac{\partial l_3}{\partial L_d} = -\frac{1}{2} \tag{75}$$

With the angle of twist at the tip defined as follows:

$$\theta_z^{\text{tip}} = \theta_z^{(3)}(l_3) = \sum_{k=1}^{n} \Phi_{9k}^{(3)}[I_k^{(3)}(l_3) + d_k^{(3)}(l_3)] \tag{76}$$

Downloaded by UNIVERSITY OF ILLINOIS on March 7, 2013 | http://arc.aiaa.org | DOI: 10.2514/1.J051244

Its partial derivatives with respect to l_m are defined as follows:

$$\frac{\partial\theta_z^{(3)}(l_3)}{\partial l_m} = \sum_{k=1}^{n}\left\{\frac{\partial\Phi_{9k}^{(3)}}{\partial l_m}[I_k^{(3)}(l_3) + d_k^{(3)}(l_3)] + \Phi_{9k}^{(3)}\left(\frac{\partial I_k^{(3)}(l_3)}{\partial l_m} + \frac{\partial d_k^{(3)}(l_3)}{\partial l_m}\right)\right\} \tag{77}$$

It can be shown that all elements of the Jordan matrix and transition matrix in different segments are not functions of l_m. Thus,

$$\frac{\partial\Phi_{9k}^{(3)}}{\partial l_m} = 0, \qquad \frac{\partial\theta_z^{(3)}(l_3)}{\partial l_m} = \sum_{k=1}^{n}\left\{\Phi_{9k}^{(3)}\left(\frac{\partial I_k^{(3)}(l_3)}{\partial l_m} + \frac{\partial d_k^{(3)}(l_3)}{\partial l_m}\right)\right\} \tag{78}$$

Derivatives

$$\frac{\partial I_k^{(m)}}{\partial l_m}$$

and

$$\frac{\partial d_k^{(m)}}{\partial l_m}$$

depend upon the matrix of functions associated with Jordan canonical form, which are defined in Appendix A.

IV. Numerical Results

A. Structural Response

In this section, we present the numerical results for an example problem. It is assumed that the crack is symmetrically placed in longitudinal direction and all three portions of the beam have at least onefold of spanwise symmetry about y–z plane. For this onefold symmetry, several geometric parameters of the cross section (such as $Q_{xy}, I_{xy}, J_{\theta x}, J_{\theta y}$, and Q_{xz}) are zero. The contour origin is taken on the axis of symmetry; thus, the warping displacement of the contour origin can be dropped. This means that the points on the contour origins along the span do not warp due to the fact that every point along the fold of symmetry is fixed. This simplifies the equation considerably to the following set:

$$-GQ_{yy}(u'' - \theta_y') = p_x \tag{79}$$

$$-E\Gamma_{zy}\phi'' - EI_{yy}\theta_y'' - GQ_{yy}(u' - \theta_y) = m_y \tag{80}$$

$$-GJ_{\theta\theta}\theta_z'' + GJ_{\theta z}\phi' = m_z \tag{81}$$

$$-E\Gamma_{zz}\phi'' - E\Gamma\theta_y'' - GJ_{\theta z}\theta_z' + GJ_{zz}\phi = -m_\omega \tag{82}$$

From this set, the equation of the beam displacement along the y–y and z–z axes are omitted, as they are uncoupled from this set and can be separately integrated. This reduced set of equations can be readily decoupled to obtain the analytical solution for each degree of freedom, as long as all distributed loadings are described as integrable functions.

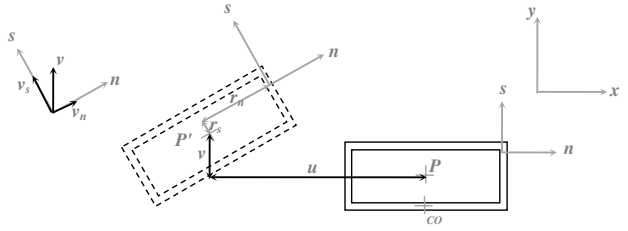

Fig. 2 Kinematics of a beam cross section.

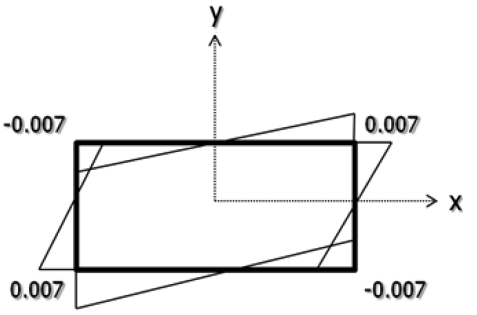

a) Closed cross-section

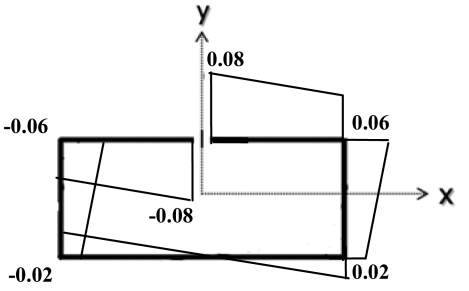

b) Open cross-section

Fig. 3 Numerical plots of warping functions.

To obtain the numerical results, the thin-walled beam is assumed to be 6 m long, with cross-sectional dimensions of 0.4 m width, 0.2 m depth, and 0.01 m thickness. The modulus of elasticity is assumed to be $E = 71.7$ GPa and $\nu = 0.33$. The numerical expressions of warping functions used herein are as follows:

$$\psi_c(s) = \begin{cases} -0.0067 + 0.033(-0.4 - s), & -0.6 \le s < -0.4 \\ 0.0067 - 0.067(-0.2 - s), & -0.4 \le s < -0.2 \\ -0.033s, & -0.2 \le s < 0.2 \\ -0.0067 + 0.067(-0.2 + s), & 0.2 \le s < 0.4 \\ 0.0067 - 0.033(-0.4 + s), & 0.4 \le s < 0.6 \end{cases} \tag{83}$$

$$\psi_o(s,n) = \begin{cases} -0.012 - 0.34(-s - 0.4) - n(s + 0.6), & -0.6 \le s < -0.4 \\ 0.028 - 0.2(-s - 0.2) - n(s + 0.06), & -0.4 \le s < -0.2 \\ -0.14s - ns, & -0.2 \le s < 0.2 \\ -0.028 + 0.2(s - 0.2) - n(s - 0.06), & 0.2 \le s < 0.4 \\ 0.0012 + 0.34(s - 0.4) - n(s - 0.6), & 0.4 \le s < 0.6 \end{cases} \tag{84}$$

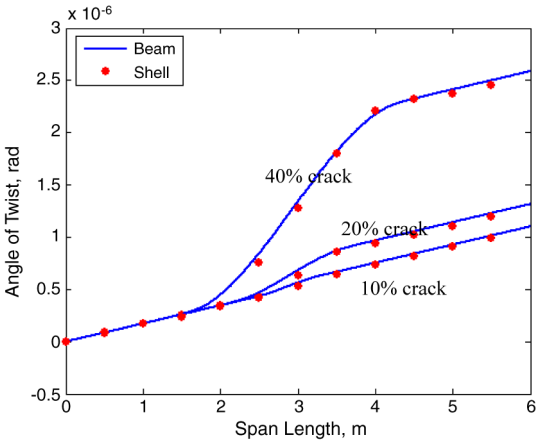

Fig. 4 Angle of twist along the beam span.

Downloaded by UNIVERSITY OF ILLINOIS on March 7, 2013 | http://arc.aiaa.org | DOI: 10.2514/1.J051244

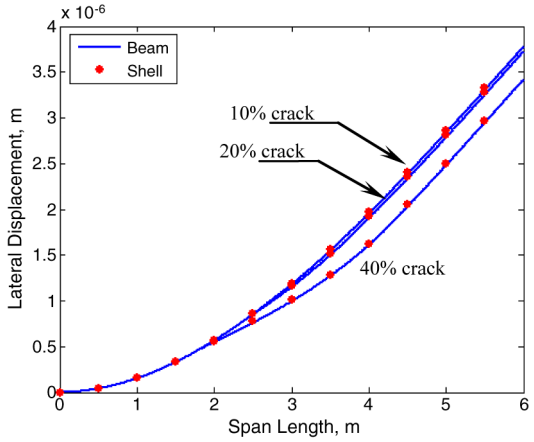

Fig. 5 Lateral deflection along the beam span.

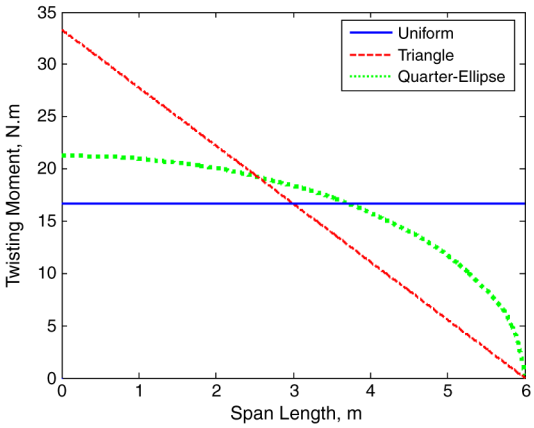

Fig. 6 Distributed twisting moment along the beam span.

These warping functions are shown in meters in Fig. 3.

For this particular section, it is found that the compatibility constants have the following values, $d_1 = d_2 = 0$, $d_3 = -0.0294$, and $d_4 = 0.122$ when the open cross section is on the right-hand side and $d_3 = 0.240$ and $d_4 = 8.16$ when the open cross section is on the left-hand side.

To verify the accuracy of the cracked thin-walled model and analytical solution approach proposed here, the numerical results of cracked beams obtained by this approach are compared with the results obtained for the same beams by the finite element analysis using the shell elements. The numerical results for the angle of twist and lateral deflection of three beams with three different crack sizes are obtained and compared. The beams are subjected to the combined loadings of a torque, $M_z = 1\ \text{N}\cdot\text{m}$, and a lateral shear force, $P_x = 1$ N, applied at the beam tip. Figure 4 shows the comparison of the angle of twist values, and Fig. 5 shows the lateral deflection values for the three cases. Each line represents a different crack size in percentage with respect to the beam length.

The results clearly show that even for large cracks, the proposed beam model yields quite accurate results for both the twist angle and deflection, compared with those obtained with shell finite elements in ABAQUS®, thus validating the accuracy of the beam model and the analytical solution.

B. Probabilistic Safety Analysis

We next show the results for the crack parameters assumed to be Gaussian random variables, with the mean and standard deviation values taken as $L_c : N(3.0, 0.5)$ for the random variable of the crack location and $L_d : N(0.6, 0.15)$ for the random variable of the crack size. The value of fraction α in Eq. (66) is assumed to be $\alpha = 0.1$. To investigate the effects of different load patterns, a study is conducted for three different cases of distributed loadings: 1) uniform distribution, 2) triangle shape, and 3) quarter-ellipse shape, as depicted in Fig. 6.

For comparison purposes, the areas under all shapes of loadings are set equal to 100 N · m. To obtain the values of the safety index β for such failure criteria, the iterative approach proposed by Rackwitz and Fiessler [12] is used. Since the limit-state function is only implicitly defined in terms of the random variables L_c and L_d, the gradients of the limit-state boundaries with respect to these variables are calculated by using the chain rule. The design-point and safety-index values converged in three iterations for all three loading cases. The final values for the design point, safety index, and probability of nonexceedance of the limit states are shown in Table 1 for this case. As both variables are Gaussian, the probability of failure is simply defined as $p_f = 1 - \Phi(\beta)$. As one would expect, the safety-index

Table 1 Final converged values of design points and safety-index values for a crack with parameters of location: L_c: $N(3.0, 0.5)$, L_d: $N(0.6, 0.15)$, and $\alpha = 0.1$

Loading type	Design-point values		Safety index	Probability of failure
	Location, L_c^*	Size, L_d^*		
Uniform	2.8268	0.74272	1.0125	15.6%
Quarter-ellipse	2.7414	0.75526	1.1571	12.4%
Triangular	2.5841	0.78151	1.4684	7.10%

Table 2 Comparison of probability-of-failure values calculated by Rackwitz–Fiessler algorithm and Monte Carlo simulation approach

Methodology	Probability of failure, %	Computation time, s
Uniform loading		
Proposed method	15.6	31.9
Monte Carlo simulation	17.4	768
Quarter-ellipse loading		
Proposed method	12.4	339
Monte Carlo simulation	11.9	2,380
Triangular loading		
Proposed method	7.10	58.8
Monte Carlo simulation	7.30	826

Table 3 Constants of the cross section

$S_{xx} = \int_A y\,\mathrm{d}A$	$J_{\theta\theta} = \int_A R_n^2\,\mathrm{d}A$
$S_{yy} = \int_A x\,\mathrm{d}A$	$J_{\theta z} = \int_A R_n \frac{\partial \psi}{\partial s}\,\mathrm{d}A$
$S_{zz} = \int_A \psi\,\mathrm{d}A$	$J_{zz} = \int_A \left(\frac{\partial \psi}{\partial s}\right)^2 \mathrm{d}A$
$\Gamma_{zz} = \int_A \psi^2\,\mathrm{d}A$	$J_{\theta x} = \int_A R_n \frac{\partial y}{\partial s}\,\mathrm{d}A$
$\Gamma_{zx} = \int_A y\psi\,\mathrm{d}A$	$J_{\theta y} = \int_A R_n \frac{\partial x}{\partial s}\,\mathrm{d}A$
$\Gamma_{zy} = \int_A x\psi\,\mathrm{d}A$	$Q_{xx} = \int_A \left(\frac{\partial y}{\partial s}\right)^2 \mathrm{d}A$
$\Gamma_{zzoc} = \int_A \psi_o \psi_c\,\mathrm{d}A$	$Q_{xy} = \int_A \frac{\partial x}{\partial s}\frac{\partial y}{\partial s}\,\mathrm{d}A$
$I_{xx} = \int_A y^2\,\mathrm{d}A$	$Q_{yy} = \int_A \left(\frac{\partial x}{\partial s}\right)^2 \mathrm{d}A$
$I_{xy} = \int_A xy\,\mathrm{d}A$	$Q_{xz} = \int_A \frac{\partial y}{\partial s}\frac{\partial \psi}{\partial s}\,\mathrm{d}A$
$I_{yy} = \int_A x^2\,\mathrm{d}A$	$Q_{yz} = \int_A \frac{\partial x}{\partial s}\frac{\partial \psi}{\partial s}\,\mathrm{d}A$

Downloaded by UNIVERSITY OF ILLINOIS on March 7, 2013 | http://arc.aiaa.org | DOI: 10.2514/1.J051244

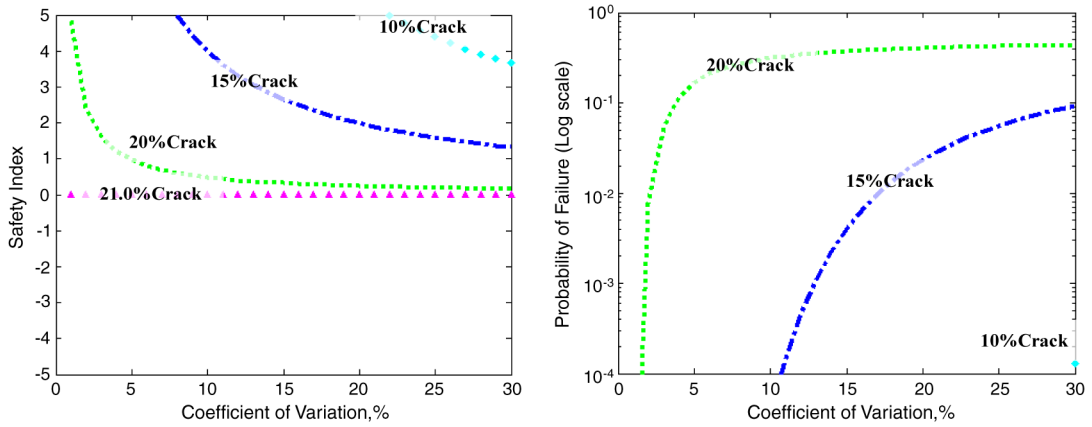

a) Safety index **b) Probability of failure**

Fig. 7 Plots of safety indices and probabilities of failure vs coefficient of variation for $\alpha = 0.3$, quarter-ellipse loading, and different mean crack sizes.

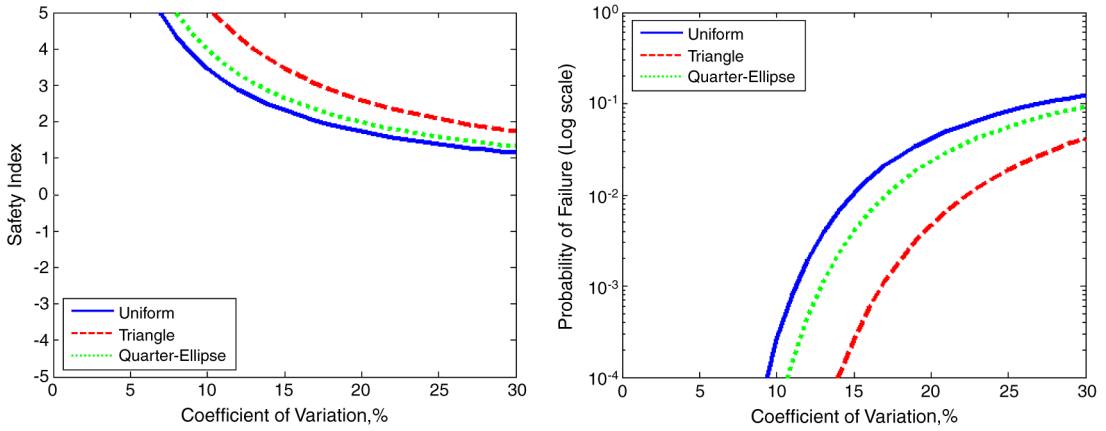

a) Safety index **b) Probability of failure**

Fig. 8 Plots of safety indices and probabilities of failure vs coefficient of variation for mean crack sizes of 15%, $\alpha = 0.3$, and three different loadings.

Downloaded by UNIVERSITY OF ILLINOIS on March 7, 2013 | http://arc.aiaa.org | DOI: 10.2514/1.J051244

value is the lowest for the uniform loading and highest for the triangular loading; the reverse is also true for the probability-of-failure values.

Table 2 shows the comparisons of the probability-of-failure values computed by the above safety-index approach and the Monte Carlo simulation. The results obtained by the proposed approach are based on three cycles of iteration, and those from the Monte Carlo approach were obtained using 500 simulations. The results demonstrate the consistency and the validation of this approach. The table also provides the computation time required by these two methods on the same computer, showing the relative computational efficiency of the safety-index approach.

In Fig. 7, we show the values of the safety index and the corresponding probabilities of failure for the case of quarter-ellipse loading for a crack location defined by parameters L_c: $N(3.0, 0.5)$ and for three crack sizes with mean values of 10, 15, and 20% and

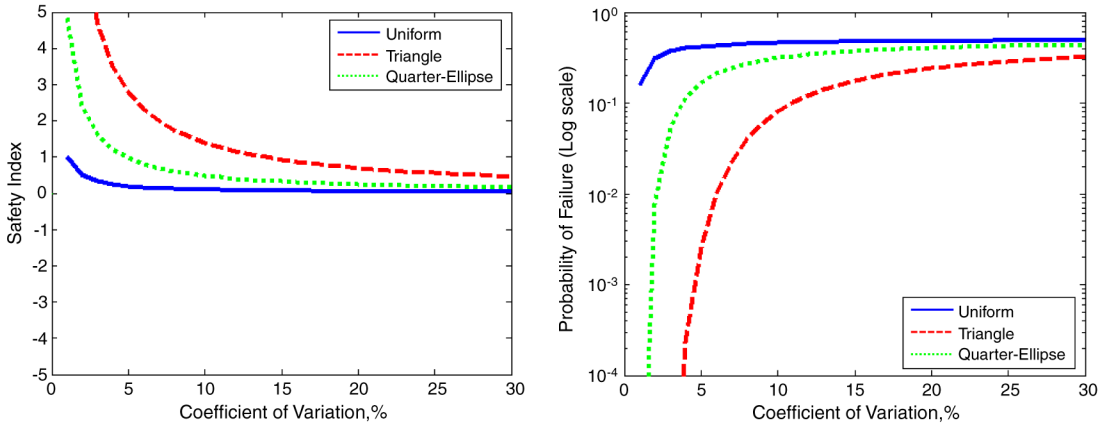

a) Safety index **b) Probability of failure**

Fig. 9 Plots of safety indices and probabilities of failure vs coefficient of variation for mean crack sizes of 20%, $\alpha = 0.3$, and three different loadings.

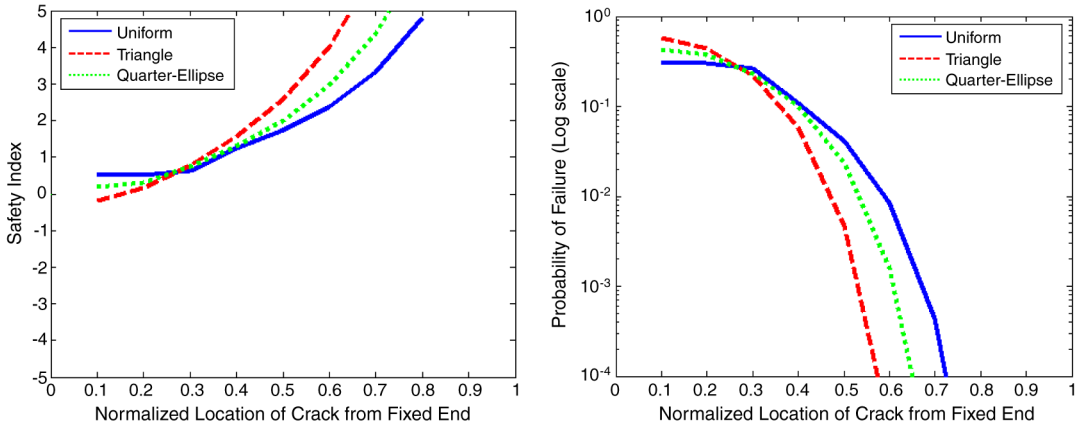

a) Safety index b) Probability of failure

Fig. 10 Plots of safety indices and probabilities of failure vs location of crack for mean crack sizes of 15%, coefficient of variation of 20%, $\alpha = 0.3$, and three different loadings.

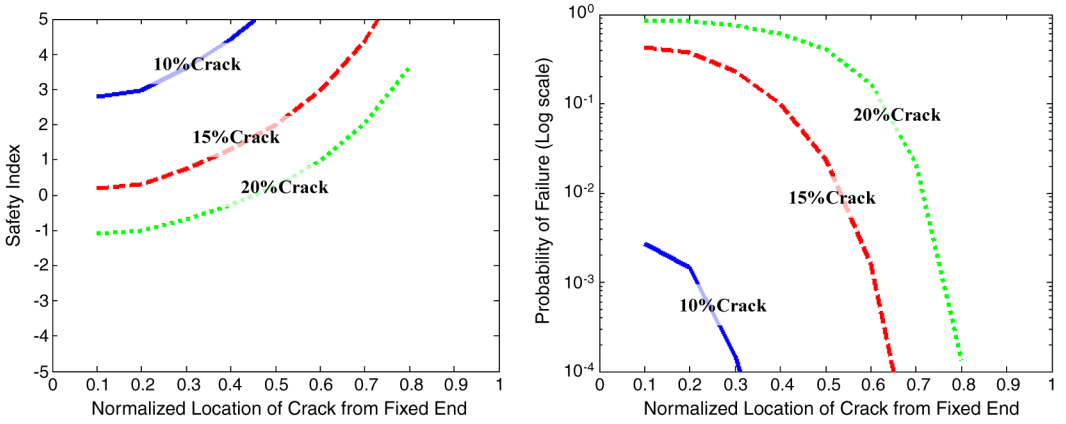

a) Safety index b) Probability of failure

Fig. 11 Plots of safety indices and probabilities of failure vs location of crack for coefficient of variation of 20%, $\alpha = 0.3$, quarter-ellipse loading, and two different mean crack sizes.

Downloaded by UNIVERSITY OF ILLINOIS on March 7, 2013 | http://arc.aiaa.org | DOI: 10.2514/1.J051244

increasing coefficients of variation. For this figure, the limit state is defined for $\alpha = 0.3$. As expected, the safety-index values decrease and the probability-of-failure values increase with the increasing coefficient of variation values. For a mean crack size of 21.0%, the probability of failure is 0.5 and the value of safety index is zero. We call this set of values the *critical mean crack-size values*. This critical crack size depends upon the value of the parameter α. For this critical value, the limit-state boundaries pass through the origin of the reduced space. For any mean crack-size values higher than the critical values, the safety-index values are negative. Also in such cases, the safety-index and the corresponding probability-of-failure values decrease with the increase in the coefficient of variation. This is because as the coefficient of variation value increases, the chances of the crack length approaching the critical length also increase, thus causing the probability of failure to increase to 0.5. These counterintuitive cases are not presented here, however. In Fig. 8, we demonstrate the values of the safety index and the corresponding probabilities of failure for three different loadings.

In the next two sets of figures, we compare the effect of the three loading patterns on the safety index and probability-of-failure values for increasing values of the coefficient of variation of the crack size. The mean location of the crack is in the middle of the beam: 3 m from the fixed end. The mean crack size in Fig. 9 is 15% of the beam length and in Fig. 10 is 20% of the beam length. Although the total torque on the beam is the same for the three loading distributions, for this selected location of the crack, the uniform loading is the most severe of the three loadings, as it leads to the lowest set of safety-index values and the highest set of probability-of-failure values.

In Fig. 10, we investigate the effect of different loading patterns on the safety-index and probability-of-failure values for different locations of crack along the beam span. For the crack size, its mean value is 15% of the beam length and its coefficient of variation is set at 20%. It is observed from the figure that both the locations of damage and the patterns of loadings do impact the values of the safety index and the corresponding probability of failure. For example, the safety index of the uniform-loading case is higher than that of quarter-ellipse loading case when the location of damage is less than a certain value around L/4 from the fixed end. This trend reverses for cracks located beyond that value near L/4.

In Fig. 11, we investigate the effect of different sizes of damage on the safety-index and probability-of-failure values for different locations of cracks along the beam span. These results are obtained for the loading pattern of quarter-ellipse. All crack sizes are assumed to have a coefficient of variation of 20%. As expected, the beam subjected to less damage possesses the higher safety index and lower probability of failure. The safety index increases and the probability of failure also decreases, as the crack is located away from the fixed end.

V. Conclusions

The paper presents an analytical approach to calculate the response of a thin-walled beam with a crack oriented along the beam length. The governing equations and associated boundary conditions of the system are derived by variational principle. The coupled equations are then expressed in a state-space form, which facilitates their uncoupling using the Jordan canonical-form approach. It is

shown that this simple thin-walled-beam model and the proposed analytical solution are able to accurately capture the effect of crack in the calculation of the beam deformations. Thus, this analytical approach can be used to study the effect of various damage parameters in a rather efficient manner. The analytical solution obtained with Jordan canonical-form approach is used in the probabilistic analysis, assuming the crack location and crack size as random variables. First-order reliability analysis is used to calculate the safety index and probability of failure for a limit state defined in terms of the angle of twist. The methodology for calculating the gradients for the limit boundary needed in the probabilistic analysis is presented. Numerical results demonstrating the application of this approach are presented for several combinations of parameters: crack size, crack-size variability, crack location, and different loading patterns. The numerical results show consistent trends, such as that a random crack near the root leads to a higher probability of failure than a crack farther away from the root, the reliability estimates depend upon the loading patterns, larger uncertainty in the crack parameters leads to larger probability of failure, etc. Such analyses can be beneficial at the preliminary design stage of an aircraft wing so that the weak point of the structure can be detected and reinforced accordingly. More important, this proposed analytical methodology can be used to verify the results obtained by comprehensive computational methods for both deterministic and nondeterministic problem scenarios.

Downloaded by UNIVERSITY OF ILLINOIS on March 7, 2013 | http://arc.aiaa.org | DOI: 10.2514/1.J051244

Appendix A: Numerical Examples of Jordan Canonical Form

In this Appendix, the details of the vectors and matrices used in the Jordan canonical-form solution of the governing equation are provided. See Table A1 for the system configuration specifications.

Since the cross section of the cracked beam in our case has onefold symmetry, only four of the six equations of equilibrium are coupled. For this case, the state-variable and force vectors are defined as follows:

$$\underline{X} = \lfloor u \quad u_1 \quad \theta_y \quad \theta_{y1} \quad \theta_z \quad \theta_{z1} \quad \phi \quad \phi_1 \rfloor^T$$

$$\underline{F} = \lfloor 0 \quad p_x \quad 0 \quad m_x \quad 0 \quad m_z \quad 0 \quad -m_w \rfloor^T$$

The state and other matrices in the state equations for the cracked and uncracked portions of the beam are defined as follows.

For the uncracked portion,

$$\underline{A} = \begin{bmatrix} 1 & 0 & 0 & 0 & 0 & 0 & 0 & 0 \\ 0 & -2.16\times10^{8} & 0 & 0 & 0 & 0 & 0 & 0 \\ 0 & 0 & 1 & 0 & 0 & 0 & 0 & 0 \\ 0 & 0 & 0 & -1.91\times10^{7} & 0 & 0 & 0 & 0 \\ 0 & 0 & 0 & 0 & 1 & 0 & 0 & 0 \\ 0 & 0 & 0 & 0 & 0 & -6.47\times10^{6} & 0 & 0 \\ 0 & 0 & 0 & 0 & 0 & 0 & 1 & 0 \\ 0 & 0 & 0 & 0 & 0 & 0 & 0 & -1.27\times10^{4} \end{bmatrix}$$

$$\underline{F} = \lfloor 0 \quad 0 \quad 0 \quad 0 \quad 0 \quad 16.67 \quad 0 \quad 0 \rfloor^T$$

The Jordan matrix $\underline{J}$, the matrix of transformation $\underline{\phi}$, and the matrix of functions $\underline{M(z)}$ can be determined following Weintraub [22]. A built-in MATLAB function called `jordan` has been used to facilitate these calculations. Derivations and comprehensive details can be found in the text by Weintraub [22]. The calculated matrices are defined as follows:

$$\underline{J} = \begin{bmatrix} 0 & 1 & 0 & 0 & 0 & 0 & 0 & 0 \\ 0 & 0 & 1 & 0 & 0 & 0 & 0 & 0 \\ 0 & 0 & 0 & 1 & 0 & 0 & 0 & 0 \\ 0 & 0 & 0 & 0 & 0 & 0 & 0 & 0 \\ 0 & 0 & 0 & 0 & 7.08 & 0 & 0 & 0 \\ 0 & 0 & 0 & 0 & 0 & -7.08 & 0 & 0 \\ 0 & 0 & 0 & 0 & 0 & 0 & 0 & 1 \\ 0 & 0 & 0 & 0 & 0 & 0 & 0 & 0 \end{bmatrix}$$

$$\underline{\Phi} = \begin{bmatrix} -11.28 & 0 & 1 & 0 & 0 & 0 & 0.23 & 0 \\ 0 & -11.28 & 0 & 1 & 0 & 0 & 0 & 0.23 \\ 0 & -11.28 & 0 & 0 & 0 & 0 & 0 & 0.23 \\ 0 & 0 & -11.28 & 0 & 0 & 0 & 0 & 0 \\ 0 & 0 & 1.13 & 0 & -0.01 & 0.01 & 1.13 & 0 \\ 0 & 0 & 1 & 1.13 & -0.06 & -0.06 & 0 & 1.13 \\ 0 & 0 & 0 & 1.13 & -0.56 & -0.56 & 0 & 1.13 \\ 0 & 0 & 0 & 0 & -3.98 & 3.98 & 0 & 0 \end{bmatrix}$$

$$\underline{M(z)} = \begin{bmatrix} 1 & z & \frac{z^2}{2} & \frac{z^3}{6} & 0 & 0 & 0 & 0 \\ 0 & 1 & z & \frac{z^2}{2} & 0 & 0 & 0 & 0 \\ 0 & 0 & 1 & z & 0 & 0 & 0 & 0 \\ 0 & 0 & 0 & 1 & 0 & 0 & 0 & 0 \\ 0 & 0 & 0 & 0 & \exp(7.08) & 0 & 0 & 0 \\ 0 & 0 & 0 & 0 & 0 & \exp(-7.08) & 0 & 0 \\ 0 & 0 & 0 & 0 & 0 & 0 & 1 & z \\ 0 & 0 & 0 & 0 & 0 & 0 & 0 & 1 \end{bmatrix}$$

For the cracked portion,

$$\underline{A} = \begin{bmatrix} 1 & 0 & 0 & 0 & 0 & 0 & 0 & 0 \\ 0 & -2.16\times10^{8} & 0 & 0 & 0 & 0 & 0 & 0 \\ 0 & 0 & 1 & 0 & 0 & 0 & 0 & 0 \\ 0 & 0 & 0 & -1.91\times10^{7} & 0 & 0 & 0 & -4.59\times10^{6} \\ 0 & 0 & 0 & 0 & 1 & 0 & 0 & 0 \\ 0 & 0 & 0 & 0 & 0 & -6.47\times10^{6} & 0 & 0 \\ 0 & 0 & 0 & 0 & 0 & 0 & 1 & 0 \\ 0 & 0 & 0 & -4.59\times10^{6} & 0 & 0 & 0 & -1.95\times10^{6} \end{bmatrix}$$

$$\underline{B} = \begin{bmatrix} 0 & 1 & 0 & 0 & 0 & 0 & 0 & 0 \\ 0 & 0 & 0 & -2.16\times10^{8} & 0 & 0 & 0 & 0 \\ 0 & 0 & 0 & 1 & 0 & 0 & 0 & 0 \\ 0 & 2.16\times10^{8} & -2.16\times10^{8} & 0 & 0 & 0 & 0 & 0 \\ 0 & 0 & 0 & 0 & 0 & 1 & 0 & 0 \\ 0 & 0 & 0 & 0 & 0 & 0 & 0 & -7.19\times10^{5} \\ 0 & 0 & 0 & 0 & 0 & 0 & 0 & 1 \\ 0 & 0 & 0 & 0 & 0 & 7.19\times10^{5} & -7.19\times10^{5} & 0 \end{bmatrix}$$

$$\underline{B} = \begin{bmatrix} 0 & 1 & 0 & 0 & 0 & 0 & 0 & 0 \\ 0 & 0 & 0 & -2.16\times10^{8} & 0 & 0 & 0 & 0 \\ 0 & 0 & 0 & 1 & 0 & 0 & 0 & 0 \\ 0 & 2.16\times10^{8} & -2.16\times10^{8} & 0 & 0 & 0 & 0 & 0 \\ 0 & 0 & 0 & 0 & 0 & 1 & 0 & 0 \\ 0 & 0 & 0 & 0 & 0 & 0 & 0 & -6.47\times10^{6} \\ 0 & 0 & 0 & 0 & 0 & 0 & 0 & 1 \\ 0 & 0 & 0 & 0 & 0 & 6.47\times10^{6} & -6.47\times10^{6} & 0 \end{bmatrix}$$

$$\underline{F} = \lfloor 0 \quad 0 \quad 0 \quad 0 \quad 0 \quad 16.67 \quad 0 \quad 0 \rfloor^{T}$$

The Jordan matrix $\underline{J}$, the matrix of transformation $\underline{\Phi}$, and the matrix of functions $\underline{M(z)}$ for this case are as follows:

$$\underline{J} = \begin{bmatrix} 0 & 1 & 0 & 0 & 0 & 0 & 0 & 0 \\ 0 & 0 & 1 & 0 & 0 & 0 & 0 & 0 \\ 0 & 0 & 0 & 1 & 0 & 0 & 0 & 0 \\ 0 & 0 & 0 & 0 & 0 & 0 & 0 & 0 \\ 0 & 0 & 0 & 0 & -0.11 & 0 & 0 & 0 \\ 0 & 0 & 0 & 0 & 0 & 0.11 & 0 & 0 \\ 0 & 0 & 0 & 0 & 0 & 0 & 0 & 1 \\ 0 & 0 & 0 & 0 & 0 & 0 & 0 & 0 \end{bmatrix}$$

$$\underline{\Phi} = \begin{bmatrix} -11.28 & 0 & 1{,}409 & 0 & 5{,}114 & -5{,}114 & 255 & 0 \\ 0 & -11.28 & 0 & 1{,}409 & -576 & -576 & 0 & 255 \\ 0 & -11.28 & 0 & 1{,}408 & -576 & -576 & 0 & 255 \\ 0 & 0 & -11.28 & 0 & 64.92 & -64.92 & 0 & 0 \\ 0 & 0 & -5{,}398 & 0 & -21{,}292 & 21{,}292 & -600 & 0 \\ 0 & 0 & 0 & -5{,}398 & 2{,}399 & 2{,}399 & 0 & -600 \\ 0 & 0 & 0 & -5{,}402 & 2{,}401 & 2401 & 0 & -600 \\ 0 & 0 & 0 & 0 & -271 & 271 & 0 & 0 \end{bmatrix}$$

$$\underline{M(z)} = \begin{bmatrix} 1 & z & \frac{z^2}{2} & \frac{z^3}{6} & 0 & 0 & 0 & 0 \\ 0 & 1 & z & \frac{z^2}{2} & 0 & 0 & 0 & 0 \\ 0 & 0 & 1 & z & 0 & 0 & 0 & 0 \\ 0 & 0 & 0 & 1 & 0 & 0 & 0 & 0 \\ 0 & 0 & 0 & 0 & \exp(-0.11) & 0 & 0 & 0 \\ 0 & 0 & 0 & 0 & 0 & \exp(0.11) & 0 & 0 \\ 0 & 0 & 0 & 0 & 0 & 0 & 1 & z \\ 0 & 0 & 0 & 0 & 0 & 0 & 0 & 1 \end{bmatrix}$$

Table A1 System configuration specifications

Parameters	Values
Section shape	Rectangular thin-walled
Section dimensions	
Width	0.4 m
Height	0.2 m
Thickness	0.01 m
Material properties	
E	71.7×10^{9} Pa,
ν	0.33
Loading type	Uniformly distributed twisting moment
Loading magnitude	16.67 N/m

Appendix B: Elements of Matrix G, and Vectors c and F_G in Eq. (65)

Matrix G, columns 1–12:

$$G(1,1{:}12) = \underline{\Phi}_1^{(1)}\underline{M(0)}^{(1)}$$

$$G(2,1{:}12) = \underline{\Phi}_3^{(1)}\underline{M(0)}^{(1)}$$

$$G(3,1{:}12) = \underline{\Phi}_5^{(1)}\underline{M(0)}^{(1)}$$

$$G(4,1{:}12) = \underline{\Phi}_7^{(1)}\underline{M(0)}^{(1)}$$

$$G(5,1{:}12) = \underline{\Phi}_9^{(1)}\underline{M(0)}^{(1)}$$

$$G(6,1{:}12) = \underline{\Phi}_{11}^{(1)}\underline{M(0)}^{(1)}$$

$$G(7,1{:}12) = \underline{\Phi}_1^{(1)}\underline{M(l_1)}^{(1)}$$

$$G(8,1{:}12) = \underline{\Phi}_3^{(1)}\underline{M(l_1)}^{(1)}$$

$$G(9,1{:}12) = [\underline{\Phi}_5^{(1)} + d_2\underline{\Phi}_{11}^{(1)}]\underline{M(l_1)}^{(1)}$$

$$G(10,1{:}12) = [\underline{\Phi}_7^{(1)} - d_3\underline{\Phi}_{11}^{(1)}]\underline{M(l_1)}^{(1)}$$

$$G(11,1{:}12) = \underline{\Phi}_9^{(1)}\underline{M(l_1)}^{(1)}$$

$$G(12,1{:}12) = d_4\underline{\Phi}_{11}^{(1)}\underline{M(l_1)}^{(1)}$$

$$G(13,1{:}12) = [GJ_{\theta y}^{(1)}\underline{\Phi}_{10}^{(1)} - GQ_{yz}^{(1)}\underline{\Phi}_{11}^{(1)} + GQ_{xy}^{(1)}(\underline{\Phi}_4^{(1)} + \underline{\Phi}_5^{(1)}) + GQ_{yy}^{(1)}(\underline{\Phi}_2^{(1)} - \underline{\Phi}_7^{(1)})]\underline{M(l_1)}^{(1)}$$

$$G(14,1{:}12) = [GJ_{\theta x}^{(1)}\underline{\Phi}_{10}^{(1)} - GQ_{xz}^{(1)}\underline{\Phi}_{11}^{(1)} + GQ_{xx}^{(1)}(\underline{\Phi}_4^{(1)} + \underline{\Phi}_5^{(1)}) + GQ_{xy}^{(1)}(\underline{\Phi}_2^{(1)} - \underline{\Phi}_7^{(1)})]\underline{M(l_1)}^{(1)}$$

Downloaded by UNIVERSITY OF ILLINOIS on March 7, 2013 | http://arc.aiaa.org | DOI: 10.2514/1.J051244

$$G(15,1{:}12) = [-E\Gamma_{zx}^{(1)}\underline{\Phi}_{12}^{(1)} + EI_{xx}^{(1)}\underline{\Phi}_{6}^{(1)} - EI_{xy}^{(1)}\underline{\Phi}_{8}^{(1)}]\underline{M(l_1)}^{(1)}$$

$$G(16,1{:}12) = [E\Gamma_{zy}^{(1)}\underline{\Phi}_{12}^{(1)} + EI_{xy}^{(1)}\underline{\Phi}_{6}^{(1)} - EI_{yy}^{(1)}\underline{\Phi}_{8}^{(1)}]\underline{M(l_1)}^{(1)}$$

$$G(17,1{:}12) = [GJ_{\theta\theta}^{(1)}\underline{\Phi}_{10}^{(1)} - GJ_{\theta z}^{(1)}\underline{\Phi}_{11}^{(1)} + GJ_{\theta x}^{(1)}(\underline{\Phi}_{4}^{(1)} + \underline{\Phi}_{5}^{(1)}) + GJ_{\theta y}^{(1)}(\underline{\Phi}_{2}^{(1)} - \underline{\Phi}_{7}^{(1)})]\underline{M(l_1)}^{(1)}$$

$$G(18,1{:}12) = [E\Gamma_{zz}^{(1)}\underline{\Phi}_{12}^{(1)} - E\Gamma_{zx}^{(1)}\underline{\Phi}_{6}^{(1)} - E\Gamma_{zy}^{(2)}\underline{\Phi}_{8}^{(1)}]\underline{M(l_1)}^{(1)}$$

Matrix G, columns 13–24:

$$G(7,13{:}24) = -\underline{\Phi}_{1}^{(2)}\underline{M(0)}^{(2)}$$

$$G(8,13{:}24) = -\underline{\Phi}_{3}^{(2)}\underline{M(0)}^{(2)}$$

$$G(9,13{:}24) = -\underline{\Phi}_{5}^{(2)}\underline{M(0)}^{(2)}$$

$$G(10,13{:}24) = -\underline{\Phi}_{7}^{(2)}\underline{M(0)}^{(2)}$$

$$G(11,13{:}24) = -\underline{\Phi}_{9}^{(2)}\underline{M(0)}^{(2)}$$

$$G(12,13{:}24) = -\underline{\Phi}_{11}^{(2)}\underline{M(0)}^{(2)}$$

$$G(13,13{:}24) = -[GJ_{\theta y}^{(2)}\underline{\Phi}_{10}^{(2)} - GQ_{yz}^{(2)}\underline{\Phi}_{11}^{(2)} + GQ_{xy}^{(2)}(\underline{\Phi}_{4}^{(2)} + \underline{\Phi}_{5}^{(2)}) + GQ_{yy}^{(2)}(\underline{\Phi}_{2}^{(2)} - \underline{\Phi}_{7}^{(2)})]\underline{M(0)}^{(2)}$$

$$G(14,13{:}24) = -[GJ_{\theta x}^{(2)}\underline{\Phi}_{10}^{(2)} - GQ_{xz}^{(2)}\underline{\Phi}_{11}^{(2)} + GQ_{xx}^{(2)}(\underline{\Phi}_{4}^{(2)} + \underline{\Phi}_{5}^{(2)}) + GQ_{xy}^{(2)}(\underline{\Phi}_{2}^{(2)} - \underline{\Phi}_{7}^{(2)})]\underline{M(0)}^{(2)}$$

$$G(15,13{:}24) = -[-E\Gamma_{zx}^{(2)}\underline{\Phi}_{12}^{(2)} + EI_{xx}^{(2)}\underline{\Phi}_{6}^{(2)} - EI_{xy}^{(2)}\underline{\Phi}_{8}^{(2)}]\underline{M(0)}^{(2)}$$

$$G(16,13{:}24) = -[E\Gamma_{zy}^{(2)}\underline{\Phi}_{12}^{(2)} + EI_{xy}^{(2)}\underline{\Phi}_{6}^{(2)} - EI_{yy}^{(2)}\underline{\Phi}_{8}^{(2)}]\underline{M(0)}^{(2)}$$

$$G(17,13{:}24) = -[GJ_{\theta\theta}^{(2)}\underline{\Phi}_{10}^{(2)} - GJ_{\theta z}^{(2)}\underline{\Phi}_{11}^{(2)} + GJ_{\theta x}^{(2)}(\underline{\Phi}_{4}^{(2)} + \underline{\Phi}_{5}^{(2)}) + GJ_{\theta y}^{(2)}(\underline{\Phi}_{2}^{(2)} - \underline{\Phi}_{7}^{(2)})]\underline{M(0)}^{(2)}$$

$$G(18,13{:}24) = -\langle d_2[-E\Gamma_{zx}^{(2)}\underline{\Phi}_{12}^{(2)} + EI_{xx}^{(2)}\underline{\Phi}_{6}^{(2)} - EI_{xy}^{(2)}\underline{\Phi}_{8}^{(2)}] + d_3[E\Gamma_{zy}^{(2)}\underline{\Phi}_{12}^{(2)} + EI_{xy}^{(2)}\underline{\Phi}_{6}^{(2)} - EI_{yy}^{(2)}] - d_4[E\Gamma_{zz}^{(2)}\underline{\Phi}_{12}^{(2)} - E\Gamma_{zx}^{(2)}\underline{\Phi}_{6}^{(2)} - E\Gamma_{zy}^{(2)}\underline{\Phi}_{8}^{(2)}]\rangle\underline{M(0)}^{(2)}$$

$$G(19,13{:}24) = \underline{\Phi}_{1}^{(2)}\underline{M(l_2)}^{(2)}$$

$$G(20,13{:}24) = \underline{\Phi}_{3}^{(2)}\underline{M(l_2)}^{(2)}$$

$$G(21,13{:}24) = [\underline{\Phi}_{5}^{(1)} + d_2\underline{\Phi}_{11}^{(1)}]\underline{M(l_2)}^{(2)}$$

$$G(22,13{:}24) = [\underline{\Phi}_{7}^{(1)} - d_3\underline{\Phi}_{11}^{(1)}]\underline{M(l_2)}^{(2)}$$

$$G(23,13{:}24) = \underline{\Phi}_{9}^{(2)}\underline{M(l_2)}^{(2)}$$

$$G(24,13{:}24) = d_4\underline{\Phi}_{11}^{(2)}\underline{M(l_2)}^{(2)}$$

$$G(25,13{:}24) = [GJ_{\theta y}^{(2)}\underline{\Phi}_{10}^{(2)} - GQ_{yz}^{(2)}\underline{\Phi}_{11}^{(2)} + GQ_{xy}^{(2)}(\underline{\Phi}_{4}^{(2)} + \underline{\Phi}_{5}^{(2)}) + GQ_{yy}^{(2)}(\underline{\Phi}_{2}^{(2)} - \underline{\Phi}_{7}^{(2)})]\underline{M(l_2)}^{(2)}$$

$$G(26,13{:}24) = [GJ_{\theta x}^{(2)}\underline{\Phi}_{10}^{(2)} - GQ_{xz}^{(2)}\underline{\Phi}_{11}^{(2)} + GQ_{xx}^{(2)}(\underline{\Phi}_{4}^{(2)} + \underline{\Phi}_{5}^{(2)}) + GQ_{xy}^{(2)}(\underline{\Phi}_{2}^{(2)} - \underline{\Phi}_{7}^{(2)})]\underline{M(l_2)}^{(2)}$$

$$G(27,13{:}24) = [-E\Gamma_{zx}^{(2)}\underline{\Phi}_{12}^{(2)} + EI_{xx}^{(2)}\underline{\Phi}_{6}^{(2)} - EI_{xy}^{(2)}\underline{\Phi}_{8}^{(2)}]\underline{M(l_2)}^{(2)}$$

$$G(28,13{:}24) = [E\Gamma_{zy}^{(2)}\underline{\Phi}_{12}^{(2)} + EI_{xy}^{(2)}\underline{\Phi}_{6}^{(2)} - EI_{yy}^{(2)}\underline{\Phi}_{8}^{(2)}]\underline{M(l_2)}^{(2)}$$

$$G(29,13{:}24) = [GJ_{\theta\theta}^{(2)}\underline{\Phi}_{10}^{(2)} - GJ_{\theta z}^{(2)}\underline{\Phi}_{11}^{(2)} + GJ_{\theta x}^{(2)}(\underline{\Phi}_{4}^{(2)} + \underline{\Phi}_{5}^{(2)}) + GJ_{\theta y}^{(2)}(\underline{\Phi}_{2}^{(2)} - \underline{\Phi}_{7}^{(2)})]\underline{M(l_2)}^{(2)}$$

$$G(30,13{:}24) = [E\Gamma_{zz}^{(2)}\underline{\Phi}_{12}^{(2)} - E\Gamma_{zx}^{(2)}\underline{\Phi}_{6}^{(2)} - E\Gamma_{zy}^{(2)}\underline{\Phi}_{8}^{(2)}]\underline{M(l_2)}^{(2)}$$

Matrix G, columns 25–36:

$$G(19,25{:}36) = \underline{\Phi}_{1}^{(3)}\underline{M(0)}^{(3)}$$

$$G(20,25{:}36) = \underline{\Phi}_{3}^{(3)}\underline{M(0)}^{(3)}$$

$$G(21,25{:}36) = \underline{\Phi}_{5}^{(3)}\underline{M(0)}^{(3)}$$

$$G(22,25{:}36) = \underline{\Phi}_{7}^{(3)}\underline{M(0)}^{(3)}$$

$$G(23,25{:}36) = \underline{\Phi}_{9}^{(3)}\underline{M(0)}^{(3)}$$

$$G(24,25{:}36) = \underline{\Phi}_{11}^{(3)}\underline{M(0)}^{(3)}$$

$$G(25,25{:}36) = -[GJ_{\theta y}^{(3)}\underline{\Phi}_{10}^{(3)} - GQ_{yz}^{(3)}\underline{\Phi}_{11}^{(3)} + GQ_{xy}^{(3)}(\underline{\Phi}_{4}^{(3)} + \underline{\Phi}_{5}^{(3)}) + GQ_{yy}^{(3)}(\underline{\Phi}_{2}^{(3)} - \underline{\Phi}_{7}^{(3)})]\underline{M(0)}^{(3)}$$

$$G(26,25{:}36) = -[GJ_{\theta x}^{(3)}\underline{\Phi}_{10}^{(3)} - GQ_{xz}^{(3)}\underline{\Phi}_{11}^{(3)} + GQ_{xx}^{(3)}(\underline{\Phi}_{4}^{(3)} + \underline{\Phi}_{5}^{(3)}) + GQ_{xy}^{(3)}(\underline{\Phi}_{2}^{(3)} - \underline{\Phi}_{7}^{(3)})]\underline{M(0)}^{(3)}$$

Downloaded by UNIVERSITY OF ILLINOIS on March 7, 2013 | http://arc.aiaa.org | DOI: 10.2514/1.J051244

$$G(27,25{:}36) = -E\Gamma^{(3)}_{zx}\underline{\Phi}^{(3)}_{12} + EI^{(3)}_{xx}\underline{\Phi}^{(3)}_{6} - EI^{(3)}_{xy}\underline{\Phi}^{(3)}_{8}]\underline{M(0)}^{(3)}$$

$$G(28,25{:}36) = -[E\Gamma^{(3)}_{zy}\underline{\Phi}^{(3)}_{12} + EI^{(3)}_{xy}\underline{\Phi}^{(3)}_{6} - EI^{(3)}_{yy}\underline{\Phi}^{(3)}_{8}]\underline{M(0)}^{(3)}$$

$$G(29,25{:}36) = -[GJ^{(3)}_{\theta\theta}\underline{\Phi}^{(3)}_{10} - GJ^{(3)}_{\theta z}\underline{\Phi}^{(3)}_{11} + GJ^{(3)}_{\theta x}(\underline{\Phi}^{(3)}_{4} + \underline{\Phi}^{(3)}_{5}) + GJ^{(3)}_{\theta y}(\underline{\Phi}^{(3)}_{2} - \underline{\Phi}^{(3)}_{7})]\underline{M(0)}^{(3)}$$

$$G(30,25{:}36) = -\langle d_2[-E\Gamma^{(3)}_{zx}\underline{\Phi}^{(3)}_{12} + EI^{(3)}_{xx}\underline{\Phi}^{(3)}_{6} - EI^{(3)}_{xy}\underline{\Phi}^{(3)}_{8}] + d_3[E\Gamma^{(3)}_{zy}\underline{\Phi}^{(3)}_{12} + EI^{(3)}_{xy}\underline{\Phi}^{(3)}_{6} - EI^{(3)}_{yy}] - d_4[E\Gamma^{(3)}_{zz}\underline{\Phi}^{(3)}_{12} - E\Gamma^{(3)}_{zx}\underline{\Phi}^{(3)}_{6} - E\Gamma^{(3)}_{zy}\underline{\Phi}^{(3)}_{8}]\rangle\underline{M(0)}^{(3)}$$

$$G(31,25{:}36) = [GJ^{(3)}_{\theta y}\underline{\Phi}^{(3)}_{10} - GQ^{(3)}_{yz}\underline{\Phi}^{(3)}_{11} + GQ^{(3)}_{xy}(\underline{\Phi}^{(3)}_{4} + \underline{\Phi}^{(3)}_{5}) + GQ^{(3)}_{yy}(\underline{\Phi}^{(3)}_{2} - \underline{\Phi}^{(3)}_{7})]\underline{M(l_3)}^{(3)}$$

$$G(32,25{:}36) = [GJ^{(3)}_{\theta x}\underline{\Phi}^{(3)}_{10} - GQ^{(3)}_{xz}\underline{\Phi}^{(3)}_{11} + GQ^{(3)}_{xx}(\underline{\Phi}^{(3)}_{4} + \underline{\Phi}^{(3)}_{5}) + GQ^{(3)}_{xy}(\underline{\Phi}^{(3)}_{2} - \underline{\Phi}^{(3)}_{7})]\underline{M(l_3)}^{(3)}$$

$$G(33,25{:}36) = [-E\Gamma^{(3)}_{zx}\underline{\Phi}^{(3)}_{12} + EI^{(3)}_{xx}\underline{\Phi}^{(3)}_{6} - EI^{(3)}_{xy}\underline{\Phi}^{(3)}_{8}]\underline{M(l_3)}^{(3)}$$

$$G(34,25{:}36) = [E\Gamma^{(3)}_{zy}\underline{\Phi}^{(3)}_{12} + EI^{(3)}_{xy}\underline{\Phi}^{(3)}_{6} - EI^{(3)}_{yy}\underline{\Phi}^{(3)}_{8}]\underline{M(l_3)}^{(3)}$$

$$G(35,25{:}36) = [GJ^{(3)}_{\theta\theta}\underline{\Phi}^{(3)}_{10} - GJ^{(3)}_{\theta z}\underline{\Phi}^{(3)}_{11} + GJ^{(3)}_{\theta x}(\underline{\Phi}^{(3)}_{4} + \underline{\Phi}^{(3)}_{5}) + GJ^{(3)}_{\theta y}(\underline{\Phi}^{(3)}_{2} - \underline{\Phi}^{(3)}_{7})]\underline{M(l_3)}^{(3)}$$

$$G(36,25{:}36) = [E\Gamma^{(3)}_{zz}\underline{\Phi}^{(3)}_{12} - E\Gamma^{(3)}_{zx}\underline{\Phi}^{(3)}_{6} - E\Gamma^{(3)}_{zy}\underline{\Phi}^{(3)}_{8}]\underline{M(l_3)}^{(3)}$$

Vector c, rows 1–12:

$$c(1{:}12,1) = [c^{(1)}_1 \;\; c^{(1)}_2 \;\; c^{(1)}_3 \;\; c^{(1)}_4 \;\; c^{(1)}_5 \;\; c^{(1)}_6 \;\; c^{(1)}_7 \;\; c^{(1)}_8 \;\; c^{(1)}_9 \;\; c^{(1)}_{10} \;\; c^{(1)}_{11} \;\; c^{(1)}_{12}]^T$$

Vector c, rows 13–24:

$$c(13{:}24,1) = [c^{(2)}_1 \;\; c^{(2)}_2 \;\; c^{(2)}_3 \;\; c^{(2)}_4 \;\; c^{(2)}_5 \;\; c^{(2)}_6 \;\; c^{(2)}_7 \;\; c^{(2)}_8 \;\; c^{(2)}_9 \;\; c^{(2)}_{10} \;\; c^{(2)}_{11} \;\; c^{(2)}_{12}]^T$$

Vector c, rows 25–36:

$$c(25{:}36,1) = [c^{(3)}_1 \;\; c^{(3)}_2 \;\; c^{(3)}_3 \;\; c^{(3)}_4 \;\; c^{(3)}_5 \;\; c^{(3)}_6 \;\; c^{(3)}_7 \;\; c^{(3)}_8 \;\; c^{(3)}_9 \;\; c^{(3)}_{10} \;\; c^{(3)}_{11} \;\; c^{(3)}_{12}]^T$$

Vector F_G, rows 1–12:

$$F_G(1,1) = -\underline{\Phi}^{(1)}_1\underline{I(0)}^{(1)}$$

$$F_G(2,1) = -\underline{\Phi}^{(1)}_3\underline{I(0)}^{(1)}$$

$$F_G(3,1) = -\underline{\Phi}^{(1)}_5\underline{I(0)}^{(1)}$$

$$F_G(4,1) = -\underline{\Phi}^{(1)}_7\underline{I(0)}^{(1)}$$

$$F_G(5,1) = -\underline{\Phi}^{(1)}_9\underline{I(0)}^{(1)}$$

$$F_G(6,1) = -\underline{\Phi}^{(1)}_{11}\underline{I(0)}^{(1)}$$

$$F_G(7,1) = \underline{\Phi}^{(2)}_1\underline{I(0)}^{(2)} - \underline{\Phi}^{(1)}_1\underline{I(l_1)}^{(1)}$$

$$F_G(8,1) = \underline{\Phi}^{(2)}_3\underline{I(0)}^{(2)} - \underline{\Phi}^{(1)}_3\underline{I(l_1)}^{(1)}$$

$$F_G(9,1) = \underline{\Phi}^{(2)}_5\underline{I(0)}^{(2)} - [\underline{\Phi}^{(1)}_5 + d_2\underline{\Phi}^{(1)}_{11}]\underline{I(l_1)}^{(1)}$$

$$F_G(10,1) = \underline{\Phi}^{(2)}_7\underline{I(0)}^{(2)} - [\underline{\Phi}^{(1)}_7 - d_3\underline{\Phi}^{(1)}_{11}]\underline{I(l_1)}^{(1)}$$

$$F_G(11,1) = \underline{\Phi}^{(2)}_9\underline{I(0)}^{(2)} - \underline{\Phi}^{(1)}_9\underline{I(l_1)}^{(1)}$$

$$F_G(12,1) = \underline{\Phi}^{(2)}_{11}\underline{I(0)}^{(2)} - d_4\underline{\Phi}^{(1)}_{11}\underline{I(l_1)}^{(1)}$$

Vector F_G, rows 13–24:

$$F_G(13,1) = [GJ^{(2)}_{\theta y}\underline{\Phi}^{(2)}_{10} - GQ^{(2)}_{yz}\underline{\Phi}^{(2)}_{11} + GQ^{(2)}_{xy}(\underline{\Phi}^{(2)}_{4} + \underline{\Phi}^{(2)}_{5}) + GQ^{(2)}_{yy}(\underline{\Phi}^{(2)}_{2} - \underline{\Phi}^{(2)}_{7})]\underline{I(0)}^{(2)} - [GJ^{(1)}_{\theta y}\underline{\Phi}^{(1)}_{10} - GQ^{(1)}_{yz}\underline{\Phi}^{(1)}_{11} + GQ^{(1)}_{xy}(\underline{\Phi}^{(1)}_{4} + \underline{\Phi}^{(1)}_{5}) + GQ^{(1)}_{yy}(\underline{\Phi}^{(1)}_{2} - \underline{\Phi}^{(1)}_{7})]\underline{I(l_1)}^{(1)}$$

$$F_G(14,1) = [GJ^{(2)}_{\theta x}\underline{\Phi}^{(2)}_{10} - GQ^{(2)}_{xz}\underline{\Phi}^{(2)}_{11} + GQ^{(2)}_{xx}(\underline{\Phi}^{(2)}_{4} + \underline{\Phi}^{(2)}_{5}) + GQ^{(2)}_{xy}(\underline{\Phi}^{(2)}_{2} - \underline{\Phi}^{(2)}_{7})]\underline{I(0)}^{(2)} - [GJ^{(1)}_{\theta x}\underline{\Phi}^{(1)}_{10} - GQ^{(1)}_{xz}\underline{\Phi}^{(1)}_{11} + GQ^{(1)}_{xx}(\underline{\Phi}^{(1)}_{4} + \underline{\Phi}^{(1)}_{5}) + GQ^{(1)}_{xy}(\underline{\Phi}^{(1)}_{2} - \underline{\Phi}^{(1)}_{7})]\underline{I(l_1)}^{(1)}$$

$$F_G(15,1) = [-E\Gamma^{(2)}_{zx}\underline{\Phi}^{(2)}_{12} + EI^{(2)}_{xx}\underline{\Phi}^{(2)}_{6} - EI^{(2)}_{xy}\underline{\Phi}^{(2)}_{8}]\underline{I(0)}^{(2)} - E\Gamma^{(1)}_{zx}\underline{\Phi}^{(1)}_{6} + EI^{(1)}_{xx}\underline{\Phi}^{(1)}_{6} - EI^{(1)}_{xy}\underline{\Phi}^{(1)}_{8}]\underline{I(l_1)}^{(1)}$$

$$F_G(16,1) = [E\Gamma^{(2)}_{zy}\underline{\Phi}^{(2)}_{12} + EI^{(2)}_{xy}\underline{\Phi}^{(2)}_{6} - EI^{(2)}_{yy}\underline{\Phi}^{(2)}_{8}]\underline{I(0)}^{(2)} - [E\Gamma^{(1)}_{zy}\underline{\Phi}^{(1)}_{12} + EI^{(1)}_{xy}\underline{\Phi}^{(1)}_{6} - EI^{(1)}_{yy}\underline{\Phi}^{(1)}_{8}]\underline{I(l_1)}^{(1)}$$

$$F_G(17,1) = [GJ^{(2)}_{\theta\theta}\underline{\Phi}^{(2)}_{10} - GJ^{(2)}_{\theta z}\underline{\Phi}^{(2)}_{11} + GJ^{(2)}_{\theta x}(\underline{\Phi}^{(2)}_{4} + \underline{\Phi}^{(2)}_{5}) + GJ^{(2)}_{\theta y}(\underline{\Phi}^{(2)}_{2} - \underline{\Phi}^{(2)}_{7})]\underline{I(0)}^{(2)} - [GJ^{(1)}_{\theta\theta}\underline{\Phi}^{(1)}_{10} - GJ^{(1)}_{\theta z}\underline{\Phi}^{(1)}_{11} + GJ^{(1)}_{\theta x}(\underline{\Phi}^{(1)}_{4} + \underline{\Phi}^{(1)}_{5}) + GJ^{(1)}_{\theta y}(\underline{\Phi}^{(1)}_{2} - \underline{\Phi}^{(1)}_{7})]\underline{I(l_1)}^{(1)}$$

$$F_G(18,1) = \langle d_2[-E\Gamma^{(2)}_{zx}\underline{\Phi}^{(2)}_{12} + EI^{(2)}_{xx}\underline{\Phi}^{(2)}_{6} - EI^{(2)}_{xy}\underline{\Phi}^{(2)}_{8}] + d_3[E\Gamma^{(2)}_{zy}\underline{\Phi}^{(2)}_{12} + EI^{(2)}_{xy}\underline{\Phi}^{(2)}_{6} - EI^{(2)}_{yy}] - d_4[E\Gamma^{(2)}_{zz}\underline{\Phi}^{(2)}_{12} - E\Gamma^{(2)}_{zx}\underline{\Phi}^{(2)}_{6} - E\Gamma^{(2)}_{zy}\underline{\Phi}^{(2)}_{8}]\rangle\underline{I(0)}^{(2)} - [E\Gamma^{(1)}_{zz}\underline{\Phi}^{(1)}_{12} - E\Gamma^{(2)}_{zx}\underline{\Phi}^{(1)}_{6} - E\Gamma^{(2)}_{zy}\underline{\Phi}^{(1)}_{8}]\underline{I(l_1)}^{(1)}$$

Downloaded by UNIVERSITY OF ILLINOIS on March 7, 2013 | http://arc.aiaa.org | DOI: 10.2514/1.J051244

$$F_G(19,1) = \underline{\Phi_2^{(3)}}\,\underline{I(0)}^{(3)} - \underline{\Phi_1^{(2)}}\,\underline{I(l_2)}^{(2)}$$

$$F_G(20,1) = \underline{\Phi_2^{(3)}}\,\underline{I(0)}^{(3)} - \underline{\Phi_3^{(2)}}\,\underline{I(l_2)}^{(2)}$$

$$F_G(21,1) = \underline{\Phi_3^{(3)}}\,\underline{I(0)}^{(3)} - [\underline{\Phi_5^{(1)}} + d_2\underline{\Phi_{11}^{(1)}}]\underline{I(l_2)}^{(2)}$$

$$F_G(22,1) = \underline{\Phi_5^{(3)}}\,\underline{I(0)}^{(3)} - [\underline{\Phi_7^{(1)}} + d_3\underline{\Phi_{11}^{(1)}}]\underline{I(l_2)}^{(2)}$$

$$F_G(23,1) = \underline{\Phi_7^{(3)}}\,\underline{I(0)}^{(3)} - \underline{\Phi_9^{(2)}}\,\underline{I(l_2)}^{(2)}$$

$$F_G(24,1) = \underline{\Phi_9^{(3)}}\,\underline{I(0)}^{(3)} - d_4\underline{\Phi_{11}^{(2)}}\,\underline{I(l_2)}^{(2)}$$

Vector F_G, rows 25–36:

$$F_G(25,1) = [GJ_{\theta y}^{(3)}\underline{\Phi_{10}^{(3)}} - GQ_{yz}^{(3)}\underline{\Phi_{11}^{(3)}} + GQ_{xy}^{(3)}(\underline{\Phi_4^{(3)}} + \underline{\Phi_5^{(3)}}) + GQ_{yy}^{(3)}(\underline{\Phi_2^{(3)}} - \underline{\Phi_7^{(3)}})]\underline{I(0)}^{(3)} - [GJ_{\theta y}^{(2)}\underline{\Phi_{10}^{(2)}} - GQ_{yz}^{(2)}\underline{\Phi_{11}^{(2)}} + GQ_{xy}^{(2)}(\underline{\Phi_4^{(2)}} + \underline{\Phi_5^{(2)}}) + GQ_{yy}^{(2)}(\underline{\Phi_2^{(2)}} - \underline{\Phi_7^{(2)}})]\underline{I(l_2)}^{(2)}$$

$$F_G(26,1) = [GJ_{\theta x}^{(3)}\underline{\Phi_{10}^{(3)}} - GQ_{xz}^{(3)}\underline{\Phi_{11}^{(3)}} + GQ_{xx}^{(3)}(\underline{\Phi_4^{(3)}} + \underline{\Phi_5^{(3)}}) + GQ_{xy}^{(3)}(\underline{\Phi_2^{(3)}} - \underline{\Phi_7^{(3)}})]\underline{I(0)}^{(3)} - [GJ_{\theta x}^{(2)}\underline{\Phi_{10}^{(2)}} - GQ_{xz}^{(2)}\underline{\Phi_{11}^{(2)}} + GQ_{xx}^{(2)}(\underline{\Phi_4^{(2)}} + \underline{\Phi_5^{(2)}}) + GQ_{xy}^{(2)}(\underline{\Phi_2^{(2)}} - \underline{\Phi_7^{(2)}})]\underline{I(l_2)}^{(2)}$$

$$F_G(27,1) = [-E\Gamma_{zx}^{(3)}\underline{\Phi_{12}^{(3)}} + EI_{xx}^{(3)}\underline{\Phi_6^{(3)}} - EI_{xy}^{(3)}\underline{\Phi_8^{(3)}}]\underline{I(0)}^{(3)} - E\Gamma_{zx}^{(2)}\underline{\Phi_{12}^{(2)}} + EI_{xx}^{(2)}\underline{\Phi_6^{(2)}} - EI_{xy}^{(2)}\underline{\Phi_8^{(2)}}]\underline{I(l_2)}^{(2)}$$

$$F_G(28,1) = [E\Gamma_{zy}^{(3)}\underline{\Phi_{12}^{(3)}} + EI_{xy}^{(3)}\underline{\Phi_6^{(3)}} - EI_{yy}^{(3)}\underline{\Phi_8^{(3)}}]\underline{I(0)}^{(3)} - [E\Gamma_{zy}^{(2)}\underline{\Phi_{12}^{(2)}} + EI_{xy}^{(2)}\underline{\Phi_6^{(2)}} - EI_{yy}^{(2)}\underline{\Phi_8^{(2)}}]\underline{I(l_2)}^{(2)}$$

$$F_G(29,1) = [GJ_{\theta\theta}^{(3)}\underline{\Phi_{10}^{(3)}} - GJ_{\theta z}^{(3)}\underline{\Phi_{11}^{(3)}} + GJ_{\theta x}^{(3)}(\underline{\Phi_4^{(3)}} + \underline{\Phi_5^{(3)}}) + GJ_{\theta y}^{(3)}(\underline{\Phi_2^{(3)}} - \underline{\Phi_7^{(3)}})]\underline{I(0)}^{(3)} - [GJ_{\theta\theta}^{(2)}\underline{\Phi_{10}^{(2)}} - GJ_{\theta z}^{(2)}\underline{\Phi_{11}^{(2)}} + GJ_{\theta x}^{(2)}(\underline{\Phi_4^{(2)}} + \underline{\Phi_5^{(2)}}) + GJ_{\theta y}^{(2)}(\underline{\Phi_2^{(2)}} - \underline{\Phi_7^{(2)}})]\underline{I(l_2)}^{(2)}$$

$$F_G(30,1) = \langle d_2[-E\Gamma_{zx}^{(3)}\underline{\Phi_{12}^{(3)}} + EI_{xx}^{(3)}\underline{\Phi_6^{(3)}} - EI_{xy}^{(3)}\underline{\Phi_8^{(3)}}] + d_3[E\Gamma_{zy}^{(3)}\underline{\Phi_{12}^{(3)}} + EI_{xy}^{(3)}\underline{\Phi_6^{(3)}} - EI_{yy}^{(3)}] - d_4[E\Gamma_{zz}^{(3)}\underline{\Phi_{12}^{(3)}} - E\Gamma_{zx}^{(3)}\underline{\Phi_6^{(3)}} - E\Gamma_{zy}^{(3)}\underline{\Phi_8^{(3)}}]\rangle\underline{I(0)}^{(3)} - [E\Gamma_{zz}^{(2)}\Phi_{12}^{(2)} - E\Gamma_{zx}^{(2)}\underline{\Phi_6^{(2)}} - E\Gamma_{zy}^{(2)}\underline{\Phi_8^{(2)}}]\underline{I(l_2)}^{(2)}$$

$$F_G(31,1) = P_x - [GJ_{\theta y}^{(3)}\underline{\Phi_{10}^{(3)}} - GQ_{yz}^{(3)}\underline{\Phi_{11}^{(3)}} + GQ_{xy}^{(3)}(\underline{\Phi_4^{(3)}} + \underline{\Phi_5^{(3)}}) + GQ_{yy}^{(3)}(\underline{\Phi_2^{(3)}} - \underline{\Phi_7^{(3)}})]\underline{I(l_3)}^{(3)}$$

$$F_G(32,1) = P_y - [GJ_{\theta x}^{(3)}\underline{\Phi_{10}^{(3)}} - GQ_{xz}^{(3)}\underline{\Phi_{11}^{(3)}} + GQ_{xx}^{(3)}(\underline{\Phi_4^{(3)}} + \underline{\Phi_5^{(3)}}) + GQ_{xy}^{(3)}(\underline{\Phi_2^{(3)}} - \underline{\Phi_7^{(3)}})]\underline{I(l_3)}^{(3)}$$

$$F_G(33,1) = M_x - E\Gamma_{zx}^{(3)}\underline{\Phi_{12}^{(3)}} + EI_{xx}^{(3)}\underline{\Phi_6^{(3)}} - EI_{xy}^{(3)}\underline{\Phi_8^{(3)}}\,\underline{I(l_3)}^{(3)}$$

$$F_G(34,1) = M_y - [E\Gamma_{zy}^{(3)}\underline{\Phi_{12}^{(3)}} + EI_{xy}^{(3)}\underline{\Phi_6^{(3)}} - EI_{yy}^{(3)}\underline{\Phi_8^{(3)}}]\underline{I(l_3)}^{(3)}$$

$$F_G(35,1) = M_z - [GJ_{\theta\theta}^{(3)}\underline{\Phi_{10}^{(3)}} - GJ_{\theta z}^{(3)}\underline{\Phi_{11}^{(3)}} + GJ_{\theta x}^{(3)}(\underline{\Phi_4^{(3)}} + \underline{\Phi_5^{(3)}}) + GJ_{\theta y}^{(3)}(\underline{\Phi_2^{(3)}} - \underline{\Phi_7^{(3)}})]\underline{I(l_3)}^{(3)}$$

$$F_G(36,1) = -M_\omega - [E\Gamma_{zz}^{(3)}\underline{\Phi_{12}^{(3)}} - E\Gamma_{zx}^{(3)}\underline{\Phi_6^{(3)}} - E\Gamma_{zy}^{(3)}\underline{\Phi_8^{(3)}}]\underline{I(l_3)}^{(3)}$$

Downloaded by UNIVERSITY OF ILLINOIS on March 7, 2013 | http://arc.aiaa.org | DOI: 10.2514/1.J051244

Acknowledgments

This work is supported by the NASA IRAC Program (agreement NNX08AC49A). Technical discussions with Technical Monitor T. Krishnamurthy (NASA Langley Research Center) are greatly appreciated.

References

[1] Benscoter, S. U., "Theory of Torsion Bending for Multicell Beams," *Journal of Applied Mechanics*, Vol. 21, No. 1, 1954, pp. 25–34.

[2] Gunnlaugsson, G. A., and Pedersen, P. T., "A Finite Element Formulation for Beams with Thin Walled Cross-Sections," *Computers and Structures*, Vol. 15, No. 6, 1982, pp. 691–699. doi:10.1016/S0045-7949(82)80011-4

[3] Pedersen, P. T., "A Beam Model for the Torsional-Bending Response of Ship Hulls," *Transactions of the Royal Institution of Naval Architects*, Vol. 125, 1982, pp. 171–182.

[4] Pedersen, P. T., "Beam Theories for Torsional-Bending Response of Ship Hulls," *Journal of Ship Research*, Vol. 35, No. 3, 1991, pp. 254–265.

[5] Shakourzadeh, H., Guo, Y. Q., and Batoz, J. L., "A Torsion Bending Element for Thin-Walled Beams with Open and Closed Cross Sections," *Computers and Structures*, Vol. 55, No. 6, 1995, pp. 1045–1054. doi:10.1016/0045-7949(94)00509-2

[6] Park, S.-W., Fujii, D., and Fujitani, Y., "A Finite Element Analysis of Discontinuous Thin-Walled Beams Considering Nonuniform Shear Warping Deformation," *Computers and Structures*, Vol. 65, No. 1, 1997, pp. 17–27. doi:10.1016/S0045-7949(96)00325-2

[7] Prokic, A., and Lukic, D., "Dynamic Analysis of Thin-Walled Closed-Section Beams," *Journal of Sound and Vibration*, Vol. 302, Nos. 4–5, 2007, pp. 962–980. doi:10.1016/j.jsv.2007.01.007

[8] Capurso, M., "Sur Calcolo Delle Travi Di Parete Sotlite in Presenta De Forze E Distorsions," *La Ricerca Scientifico*, Vol. 6, 1964, pp. 213–286.

[9] Prokic, A., "Thin-Walled Beams with Open and Closed Cross-Sections," *Computers and Structures*, Vol. 47, No. 6, 1993, pp. 1065–1070. doi:10.1016/0045-7949(93)90310-A

[10] Rackwitz, R., *Practical Probabilistic Approach to Design*, Tech. Univ. of Munich, Munich, 1976.

[11] Rackwitz, R., and Fiessler, B., *Note on Discrete Safety Checking When Using Non-Normal Stochastic Models for Basic Variables*, Massachusetts Inst. of Technology, Cambridge, MA, 1976.

[12] Rackwitz, R., and Fiessler, B., "Structural Reliability Under Combined Random Load Sequences," *Computers and Structures*, Vol. 9, No. 5, 1978, pp. 489–494. doi:10.1016/0045-7949(78)90046-9

[13] Ang, A. H.-S., and Tang, W. H., *Probability Concepts in Engineering Planning and Design: Decision, Risk and Reliability*, Vol. 2, Wiley, New York, 1984.

[14] Haldar, A., and Mahadevan, S., *Probability, Reliability and Statistical Methods in Engineering Design*, Wiley, New York, 2000.

[15] Fiessler, B., Neumann, H.-J., and Rackwitz, R., "Quadratic Limit States in Structural Reliability," Vol. 105, No. 4, 1979, pp. 661–676.

[16] Rahman, S., and Kim, J. S., "Probabilistic Fracture Mechanics for Nonlinear Structures," *International Journal of Pressure Vessels and Piping*, Vol. 78, No. 4, 2001, pp. 261–269. doi:10.1016/S0308-0161(01)00006-0

[17] Huh, J., and Haldar, A., "Stochastic Finite-Element-Based Seismic Risk of Nonlinear Structures," *Journal of Structural Engineering*, Vol. 127, No. 3, 2001, pp. 323–329.

doi:10.1061/(ASCE)0733-9445(2001)127:3(323)
[18] Kapania, R. K., and Castel, F., "Simple Element for Aeroelastic Analysis of Undamaged and Damaged Wings," *AIAA Journal*, Vol. 28, No. 2, 1990, pp. 329–337. doi:10.2514/3.10393
[19] Krishnamurthy, T., and Tsai, F. J., "Static and Dynamic Structural Response of an Aircraft Wing with Damage Using Equivalent Plate Analysis," AIAA/ASME/ASCE/AHS/ASC Structures, Structural Dynamics and Materials Conference, AIAA Paper 2008-1967, 2008.
[20] Dang, T. D., Kapania, R. K., and Patil, M. J., "Analytical Modeling of Cracked Thin-Walled Beams Under Torsion," *AIAA Journal*, Vol. 48, No. 3, 2010, pp. 664–675. doi:10.2514/1.45393
[21] Librescu, L., and Song, O., *Thin-Walled Composite Beams: Theory and Application*, Springer, Dordrecht, The Netherlands, 2006.
[22] Weintraub, S. H., *Jordan Canonical Form : Theory and Practice*, Morgan & Claypool, San Rafael, CA, 2009.

A. Pelegri
Associate Editor

Downloaded by UNIVERSITY OF ILLINOIS on March 7, 2013 | http://arc.aiaa.org | DOI: 10.2514/1.J051244